Acknowledgements

To begin, I wish to thank Katja Lindenberg for inviting me to write this book for the Springer INLS Series. The first edition of this book, which appeared in 1992, was the result of lectures on classical and quantum chaos theory that I gave at the Institute for Nonlinear Science, University of California, San Diego, in 1987, and later at Guangxi Normal University in Guilin, China, and at the University of Texas in Austin, Texas. The first edition focused on classical chaos theory and the manifestations of chaos in bounded quantum systems. This new edition contains selected material from the first edition but also discusses the manifestations of chaos in open systems, which has been a major focus of the field in recent years. The new edition also contains a thorough grounding in random matrix theory and supersymmetry techniques, which have become essential for analyzing properties of quantum systems whose classical counterpart is chaotic.

As before, I have attempted to write the book both as a textbook and as a research resource. Because it was necessary to keep the book a reasonable length, I have made a judgment about the material that I use to illustrate ideas, but at the same time I have tried to reference all other relevant work that I know about.

This book has benefited from discussions with many colleagues and students in the fields of classical and quantum chaos over the years. I hope I have done justice to the contributions they have all made to this important field of dynamics.

Linda Reichl
The University of Texas at Austin
March 2003

2
Fundamental Concepts

2.1 Introduction

There are three basic concepts that are essential for understanding the dynamical behavior of nonlinear conservative systems. The first is the concept of *global symmetries*, which serve to constrain the dynamical flow of the system to lower-dimensional surfaces in the phase space. Some of these global symmetries are obvious and are related to the space-time symmetries of the system. Others are not obvious and have been called *hidden symmetries* by Moser [Moser 1979]. When there are as many global symmetries as degrees of freedom, the dynamical system is said to be *integrable*. The second important concept is that of *nonlinear resonance*. As Kolmogorov [Kolmogorov 1954], Arnol'd [Arnol'd 1963], and Moser [Moser 1962] have shown, when a small symmetry-breaking term is added to the Hamiltonian, most of the phase space continues to behave as if the symmetries still exist. However, in regions where the symmetry-breaking term allows resonance to occur between otherwise uncoupled degrees of freedom, the dynamics begins to change its character. When resonances do occur, they generally occur on all scales in the phase space and give rise to an incredibly complex structure, as we shall see. The third important concept is that of *chaos* or *sensitive dependence on initial conditions*. For the class of systems in which symmetries can be broken by adding small symmetry-breaking terms, chaos first appears in the neighborhood of the nonlinear resonances. As the strength of the symmetry-breaking term increases and

the size of the resonance regions increases, ever larger regions of the phase space become chaotic.

As we shall show in Sect. 2.2, the dynamical evolution of systems with broken symmetry cannot be determined using conventional perturbation theory, because of the existence of nonlinear resonances. This occurs because nonlinear resonances cause a topological change locally in the structure of the phase space, and conventional perturbation theory is not adequate to deal with such topological changes.

In Sect. 2.3, we introduce the concept of integrability. A system is integrable if it has as many global constants of the motion as degrees of freedom. The connection between global symmetries and global constants of motion was first proven for dynamical systems by Noether [Noether 1918]. We will give a simple derivation of Noether's theorem in Sect. 2.3. In Sect. 2.3, we illustrate these methods for the simple three-body Toda lattice. It is usually impossible to tell if a system is integrable or not just by looking at the equations of motion. The Poincaré surface of section provides a very useful numerical tool for testing for integrability and will be used throughout the remainder of this book. We will illustrate the use of the Poincaré surface of section for the classic model of Henon and Heiles [Henon and Heiles 1964].

In Sect. 2.4, we introduce the concept of nonlinear resonances and illustrate their behavior for some simple models originally introduced by Walker and Ford [Walker and Ford 1969]. These models are interesting because they show that resonances may appear or disappear as parameters of the system are varied and the overlap of nonlinear resonances leads to the onset of chaos. Conventional perturbation theory does not work when nonlinear resonances are present. But Kolmogorov, Arnol'd, and Moser (collectively called KAM) have developed a rapidly converging perturbation theory that can be used to describe nonresonant regions of the phase space, precisely because it is constructed to avoid the resonance regions. KAM perturbation theory will be described in Sect. 2.5.

In practice, chaos is defined in terms of the dynamical behavior of pairs of orbits that initially are close together in the phase space. If the orbits move apart exponentially in any direction in the phase space, the flow is said to be chaotic. The rate of exponential divergence of pairs of orbits is measured by the so-called Lyapounov exponents. There will be one such exponent for each dimension in the phase space. If all the Lyapounov exponents are zero, the dynamical flow is regular. If even one exponent is positive, the flow will be chaotic. A detailed discussion of the behavior of Lyapounov exponents for conservative systems is given in Sect. 2.6 and is illustrated in terms of the Henon-Heiles system. Systems with positive Lyapounov exponents also have positive KS metric entropy. The KS metric entropy is defined in Sect. 2.6 and computed for the baker's transformation, one of the simplest known chaotic dynamical systems.

Much of the work done on the transition to chaos in conservative systems has been done on one degree of freedom conservative systems driven

by a time-periodic external field. Such systems are conservative in a higher-dimensional phase space and are volume-preserving. They are particularly easy to study both analytically and numerically because the location of resonances is largely determined by the structure of the unperturbed system, and Poincaré surfaces of section are strobe plots. In Sect. 2.7, we describe the mechanism by which chaos occurs in the conservative Duffing system, which consists of a particle in a double well potential driven by a monochromatic external time-periodic field. We will see clearly why a chaotic region (stochastic layer) always forms at the separatrix of nonlinear resonance zones in nonintegrable systems.

2.2 Conventional Perturbation Theory

Historically, the difficulties in obtaining long-time predictions for the evolution of mechanical systems was brought into focus with Poincare's proof that conventional perturbation expansions generally diverge and cannot be used as a tool to provide long-time prediction. In order to build some intuition concerning the origin of these divergences, let us consider a system with two degrees of freedom having a Hamiltonian $H_0(p_1, p_2, q_1, q_2)$, which after a canonical transformation can be written in terms of action-angle variables $(J_1, J_2, \theta_1, \theta_2)$ in the form $H_0(J_1, J_2)$. For example, the Hamiltonian for the relative motion of a moon of mass m_1, orbiting a planet of mass m_2 (the Kepler system), can be written

$$H_0 = \frac{{p_r}^2}{2\mu} + \frac{{p_\phi}^2}{2\mu r^2} - \frac{k}{r} = E, \tag{2.2.1}$$

where (p_r, p_ϕ) and (r, ϕ) are the relative momentum and positions, respectively, of the two bodies in polar coordinates, E is the total energy of the system, $\mu = \frac{m_1 m_2}{m_1 + m_2}$ is the reduced mass, and $k = G m_1 m_2$ (G is the gravitational constant). The total angular momentum, $\mathbf{L}$, is conserved for this problem so the plane of motion, (r, ϕ), is taken to lie in the plane perpendicular to $\mathbf{L}$. After a canonical transformation from coordinates (p_r, p_ϕ, r, ϕ) to action-angle coordinates $(J_1, J_2, \theta_1, \theta_2)$, the Hamiltonian takes the form [Goldstein 1980]

$$H_0 = \frac{-\mu k^2}{2(J_1 + J_2)^2} = E. \tag{2.2.2}$$

The motion is fairly complicated (elliptic or hyperbolic orbits) in terms of coordinates (p_r, p_ϕ, r, ϕ), but in terms of action-angle coordinates it is simple. Hamilton's equations of motion yield

$$\frac{dJ_i}{dt} = -\frac{\partial H_0}{\partial \theta_i} = 0 \tag{2.2.3}$$

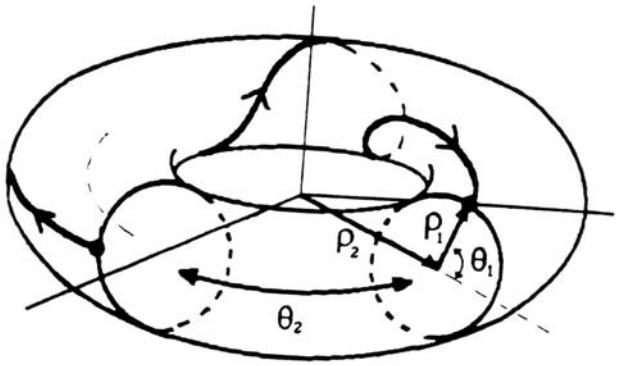

Figure 2.2.1. For integrable systems with two degrees of freedom, each trajectory lies on a torus constructed from the action-angle variables $(J_1, J_2, \theta_1, \theta_2)$. The radii of the torus are $\rho_i = \sqrt{2J_i}$ for $i = (1, 2)$. If the frequencies $\omega_i = \frac{d\theta_i}{dt}$ $(i = 1, 2)$ are commensurate, the trajectory will be periodic. If the frequencies are incommensurate, the trajectory will never repeat.

and

$$\frac{d\theta_i}{dt} = \frac{\partial H_0}{\partial J_i} = \omega_i(J_1, J_2), \tag{2.2.4}$$

where $i = (1, 2)$ and t is the time. Thus, we find that

$$J_i = c_i \tag{2.2.5}$$

and

$$\theta_i = \omega_i t + d_i, \tag{2.2.6}$$

where c_i and d_i are constants determined by the initial conditions. We see immediately that the energy of this system is constant. It is useful to picture the motion of this system as lying on a torus as shown in Fig. 2.2.1. The torus will have two constant radii, which we define as $\rho_i = \sqrt{2J_i}$ for $i = (1, 2)$, and two angular variables (θ_1, θ_2). A single orbit of the Kepler system will evolve on this torus according to Eqs. (2.2.5) and (2.2.6). Notice that there are two frequencies associated with this system, ω_1 and ω_2. If these two frequencies are commensurate (that is, if $m\omega_1 = n\omega_2$, where m and n are integers), then the trajectory will be periodic and the orbit will repeat itself. If the two frequencies are incommensurate (irrational multiples of one another), then the trajectory will never repeat itself as it moves around the torus and eventually will cover the entire surface of the torus. Note also that the frequencies themselves depend on the action variables and therefore on the energy of the system. This is a characteristic feature of a nonlinear system.

Let us now assume that a perturbation acts in the plane of motion due to the presence of another planet. We shall treat this perturbation as an

external field. In the presence of this perturbation, the Hamiltonian will take the form

$$H = H_0(J_1, J_2) + \epsilon V(J_1, J_2, \theta_1, \theta_2), \tag{2.2.7}$$

where ϵ is a small parameter, $\epsilon \ll 1$. We wish to find corrections to the unperturbed trajectories, $J_i = c_i$, due to the perturbation. Since we cannot solve the new equations of motion exactly, we can hope to obtain approximate solutions using perturbation expansions in the small parameter ϵ. Let's try it. First we note that since we are dealing with periodic bound state motion, we can expand the perturbation in a Fourier series. We then write the Hamiltonian in Eq. (2.2.7) in the form

$$H = H_0(J_1, J_2) + \epsilon \sum_{n_1=-\infty}^{\infty} \sum_{n_2=-\infty}^{\infty} V_{n_1,n_2}(J_1, J_2) \cos(n_1\theta_1 + n_2\theta_2). \tag{2.2.8}$$

Next, we introduce a generating function, $G(\mathcal{J}_1, \mathcal{J}_2, \theta_1, \theta_2)$, which we define as

$$G(\mathcal{J}_1, \mathcal{J}_2, \theta_1, \theta_2) = \mathcal{J}_1\theta_1 + \mathcal{J}_2\theta_2 + \epsilon \sum_{n_1=-\infty}^{\infty} \sum_{n_2=-\infty}^{\infty} g_{n_1,n_2}(\mathcal{J}_1, \mathcal{J}_2) \sin(n_1\theta_1 + n_2\theta_2), \tag{2.2.9}$$

where g_{n_1,n_2} will be determined below. The generating function in Eq. (2.2.9) generates a canonical transformation from the set of action-angle variables, $(J_1, J_2, \theta_1, \theta_2)$, to a new set of canonical action-angle variables, $(\mathcal{J}_1, \mathcal{J}_2, \Theta_1, \Theta_2)$, via the following equations [Goldstein 1980]:

$$J_i = \frac{\partial G}{\partial \theta_i} = \mathcal{J}_i + \epsilon \sum_{n_1=-\infty}^{\infty} \sum_{n_2=-\infty}^{\infty} n_i g_{n_1,n_2} \cos(n_1\theta_1 + n_2\theta_2) \tag{2.2.10}$$

and

$$\Theta_i = \frac{\partial G}{\partial \mathcal{J}_i} = \theta_i + \epsilon \sum_{n_1=-\infty}^{\infty} \sum_{n_2=-\infty}^{\infty} \frac{\partial g_{n_1,n_2}}{\partial \mathcal{J}_i} \sin(n_1\theta_1 + n_2\theta_2). \tag{2.2.11}$$

The new Hamiltonian, $H'(\mathcal{J}_1, \mathcal{J}_2, \Theta_1, \Theta_2)$, is obtained from Eq. (2.2.8) by solving Eqs. (2.2.10) and (2.2.11) for (J_i, θ_i) as a function of $(\mathcal{J}_i, \Theta_i)$ and plugging into Eq. (2.2.8). If we do that and then expand $H'(\mathcal{J}_1, \mathcal{J}_2, \Theta_1, \Theta_2)$ in a Taylor series in the small parameter ϵ, we find

$$\begin{aligned} &H'(\mathcal{J}_1, \mathcal{J}_2, \Theta_1, \Theta_2) \\ &\quad = H_0'(\mathcal{J}_1, \mathcal{J}_2) + \epsilon \sum_{n_1=-\infty}^{\infty} \sum_{n_2=-\infty}^{\infty} (n_1\omega_1 + n_2\omega_2) g_{n_1,n_2} \cos(n_1\Theta_1 + n_2\Theta_2) \\ &\qquad + \epsilon \sum_{n_1=-\infty}^{\infty} \sum_{n_2=-\infty}^{\infty} V_{n_1,n_2}(\mathcal{J}_1, \mathcal{J}_2) \cos(n_1\Theta_1 + n_2\Theta_2) + O(\epsilon^2), \end{aligned} \tag{2.2.12}$$

where

$$\omega_i = \frac{\partial H'_o}{\partial \mathcal{J}_i}. \tag{2.2.13}$$

Now remove terms of order ϵ by choosing

$$g_{n_1,n_2} = -\frac{V_{n_1,n_2}(\mathcal{J}_1, \mathcal{J}_2)}{(n_1\omega_1 + n_2\omega_2)}. \tag{2.2.14}$$

Then

$$H'(\mathcal{J}_1, \mathcal{J}_2, \Theta_1, \Theta_2) = H'_o(\mathcal{J}_1, \mathcal{J}_2) + O(\epsilon^2) \tag{2.2.15}$$

and

$$J_i = \mathcal{J}_i - \epsilon \sum_{n_1=-\infty}^{\infty} \sum_{n_2=-\infty}^{\infty} \frac{n_i V_{n_1,n_2} \cos(n_1\Theta_1 + n_2\Theta_2)}{(n_1\omega_1 + n_2\omega_2)} + O(\epsilon^2). \tag{2.2.16}$$

To lowest order in ϵ, this is the solution to the problem. New actions, $\mathcal{J}_i$, have been obtained that contain corrections due to the perturbation. If, for example, $\epsilon = 0.01$, then by retaining only first-order corrections we neglect terms of order $\epsilon^2 = 0.0001$. To first order in ϵ, $\mathcal{J}_i$ is a constant and Θ_i varies linearly in time. This is the hope. However, there is a catch. For any of this to have meaning, we must have

$$|n_1\omega_1 + n_2\omega_2| \gg \epsilon V_{n_1,n_2}. \tag{2.2.17}$$

But the condition in Eq. (2.2.17) breaks down when internal nonlinear resonances occur and cause the perturbation expansion to diverge. Poincaré showed that it is a general property of perturbation expansions of this type that they can be expected to diverge.

2.3 Integrability

A concept that is essential to the remainder of this book is that of integrability. Let us consider a system with N degrees of freedom. Its phase space has $2N$ dimensions. Such a system is *integrable* if there exist N independent isolating integrals of motion, I_i, such that

$$I_i(p_1, \ldots, p_N, q_1, \ldots, q_N) = C_i, \tag{2.3.1}$$

for $i = 1, \ldots, N$, where C_i is a constant and p_i and q_i are the canonical momentum and position associated with the ith degree of freedom. The functions I_i are independent if their differentials, dI_i, are linearly independent. It is important to distinguish between isolating and nonisolating integrals [Wintner 1947]. Nonisolating integrals (an example is the initial coordinates of a trajectory) generally vary from trajectory to trajectory and usually do not provide useful information about a system. On the other hand, isolating integrals of motion, by Noether's theorem, are due to

symmetries (some "hidden") of the dynamical system and define surfaces in phase space.

The condition for integrability may be put in another form. A classical system with N degrees of freedom is integrable if there exist N independent globally defined functions, $I_i(p_1, \ldots, p_N, q_i, \ldots, q_N)$, for $i = 1, \ldots, N$, whose mutual Poisson brackets (see Appendix A.4) vanish,

$$\{I_i, I_j\}_{Poisson} = 0, \tag{2.3.2}$$

for $i = 1, \ldots, N$ and $j = 1, \ldots, N$. Then the quantities I_i form a set of N phase space coordinates. In conservative systems, the Hamiltonian, $H(p_1, \ldots, p_N, q_1, \ldots, q_N)$, will be one of the constants of the motion. In general, the equation of motion of a phase function, $f = f(p_1, \ldots, p_N, q_1, \ldots, q_N, t)$, is given by

$$\frac{df}{dt} = \frac{\partial f}{\partial t} + \{H, f\}_{Poisson}. \tag{2.3.3}$$

Thus Eqs. (2.3.2) and (2.3.3) imply that $\frac{dI_i}{dt} = 0$. If a system is integrable, there are no internal nonlinear resonances leading to chaos. All orbits lie on N-dimensional surfaces in the $2N$-dimensional phase space.

2.3.1 Noether's Theorem

As was shown by Noether [Noether 1918], isolating integrals result from symmetries. For example, the total energy is an isolating integral (is a constant of the motion) for systems that are homogeneous in time (invariant under a translation in time). Total angular momentum is an isolating integral for systems that are isotropic in space.

Noether's theorem is generally formulated in terms of the Lagrangian (see [Goldstein 1980] and Appendix A). Let us consider a dynamical system with N degrees of freedom whose state is given by the set of generalized velocities and positions $(\{\dot{q}_i\}, \{q_i\})$. Let us consider a system whose Lagrangian, $L = L(\{\dot{q}_i\}, \{q_i\})$, is known. For simplicity, we consider a system with a time-independent Lagrangian. The equations of motion are given by the Lagrange equations

$$\frac{\partial L}{\partial q_i} - \frac{d}{dt}\left(\frac{\partial L}{\partial \dot{q}_i}\right) = 0, \quad (i = 1, \ldots, N). \tag{2.3.4}$$

For such systems, Noether's theorem may be stated as follows.

•*Noether's theorem*

If a transformation

$$t \to t' = t + \delta t, \quad q_i(t) \to q_i'(t') = q_i(t) + \delta q_i(t), \quad \text{and}$$
$$\dot{q}_i \to \dot{q}_i'(t') = \dot{q}_i(t) + \delta \dot{q}_i(t)$$

(for $i = 1, \ldots, N$) leaves the Lagrangian form invariant,

$$L(\{\dot{q}_i(t)\}, \{q_i(t)\}) \to L'(\{\dot{q}'_i(t')\}, \{q'_i(t')\}) = L(\{\dot{q}'_i(t')\}, \{q'_i(t')\}), \quad (2.3.5)$$

and leaves the action integral invariant

$$\int_{t'_1}^{t'_2} dt' L(\{\dot{q}'_i(t')\}, \{q'_i(t')\}) - \int_{t_1}^{t_2} dt L(\{\dot{q}_i(t)\}, \{q_i(t)\}) = 0, \quad (2.3.6)$$

then there exists an isolating integral of motion associated with this symmetry transformation. •

Before we proceed to show this, we must distinguish between variations of the coordinates at a fixed time, $q_i(t) \to q'_i(t) = q_i(t) + \delta Q_i(t)$ and variations at a later time (as we indicated above) $q_i(t) \to q'_i(t') = q_i(t) + \delta q_i(t)$. $\delta q_i(t)$ is a convective variation and differs from $\delta Q_i(t)$ by a convective term, $\delta q_i(t) = \delta Q_i(t) + \dot{q}_i \delta t$ [Reichl 1998].

•*Proof of Noether's theorem*

Let us write Eq. (2.3.6) in the form

$$\int_{t_1+\delta t_1}^{t_2+\delta t_2} dt\ L(\{\dot{q}'_i(t)\}, \{q'_i(t)\}) - \int_{t_1}^{t_2} dt\ L(\{\dot{q}_i(t)\}, \{q_i(t)\}) = 0, \quad (2.3.7)$$

where on the leftmost integral we have let the dummy variable $t' \to t$. Next let $\{\dot{q}'_i(t)\} = \{\dot{q}_i(t) + \delta \dot{Q}_i(t)\}$ and $\{q'_i(t)\} = \{q_i(t) + \delta Q_i(t)\}$, and expand the integral to first order in the variations. We then find

$$\int_{t_1+\delta t_1}^{t_2+\delta t_2} dt \left\{ L(\{\dot{q}_i(t)\}, \{q_i(t)\}) + \sum_{i=1}^{N} \left[\left(\frac{\partial L}{\partial \dot{q}_i} \right) \delta \dot{Q}_i + \left(\frac{\partial L}{\partial q_i} \right) \delta Q_i \right] \right\}$$
$$- \int_{t_1}^{t_2} dt L(\{\dot{q}_i(t)\}, \{q_i(t)\}) = 0. \quad (2.3.8)$$

If we next keep only first-order contributions in the variations in the limits of integration, we find

$$\int_{t_1}^{t_2} dt \left\{ \sum_{i=1}^{N} \left[\left(\frac{\partial L}{\partial \dot{q}_i} \right) \delta \dot{Q}_i + \left(\frac{\partial L}{\partial q_i} \right) \delta Q_i \right] \right\}$$
$$+ \delta t_2 L(t_2) - \delta t_1 L(t_1) = 0, \quad (2.3.9)$$

where $L(t_k) = L(\{\dot{q}_i(t_k)\}, \{q_i(t_k)\})$. Equation (2.3.9) can now be rewritten in the form

$$\int_{t_1}^{t_2} dt \left\{ \frac{d}{dt}(\delta t L) + \sum_{i=1}^{N} \left[\left(\frac{\partial L}{\partial \dot{q}_i} \right) \delta \dot{Q}_i + \left(\frac{\partial L}{\partial q_i} \right) \delta Q_i \right] \right\}. \quad (2.3.10)$$

Let us now make use of Lagrange's Eqs. (2.3.4) and note that $\delta\dot{Q}_i = \frac{d}{dt}\delta Q_i$. Then, after some rearrangement of terms, we find

$$\int_{t_1}^{t_2} dt \frac{d}{dt}\left\{ L\delta t + \sum_{i=1}^{N}\left(\frac{\partial L}{\partial \dot{q}_i}\right)\delta Q_i \right\} = 0. \tag{2.3.11}$$

Let us now rewrite Eq. (2.3.11) in terms of our convective variations. We then find

$$\int_{t_1}^{t_2} dt \frac{d}{dt}\left\{ \left[L - \sum_{i=1}^{N}\dot{q}_i\left(\frac{\partial L}{\partial \dot{q}_i}\right)\right]\delta t + \sum_{i=1}^{N}\left(\frac{\partial L}{\partial \dot{q}_i}\right)\delta q_i \right\} = 0. \tag{2.3.12}$$

Thus

$$\frac{d}{dt}\left\{ \left[L - \sum_{i=1}^{N}\dot{q}_i\left(\frac{\partial L}{\partial \dot{q}_i}\right)\right]\delta t + \sum_{i=1}^{N}\left(\frac{\partial L}{\partial \dot{q}_i}\right)\delta q_i \right\} = 0, \tag{2.3.13}$$

and we have obtained an isolating integral as a result of our symmetry transformation. •

To illustrate the use of Eq. (2.3.13), let us consider some examples. Assume that we translate the system in time by a constant amount, $\delta t = \epsilon$, but let $\delta q_i = 0$. Then we have

$$\frac{d}{dt}\left\{ L - \sum_{i=1}^{N}\dot{q}_i\left(\frac{\partial L}{\partial \dot{q}_i}\right)\right\} = \frac{dH}{dt} = 0 \tag{2.3.14}$$

since the quantity in curly brackets is the Hamiltonian (see Appendix A). Thus homogeneity in time gives rise to the Hamiltonian as an isolating integral and to energy conservation. Suppose that we let $\delta t = 0$ but translate one coordinate, q_j, by a constant amount, $\delta q_i = \epsilon\delta_{i,j}$, where $\delta_{i,j}$ is the Kronecker delta. Then we find

$$\frac{d}{dt}\left(\frac{\partial L}{\partial \dot{q}_j}\right) = \frac{dp_j}{dt} = 0. \tag{2.3.15}$$

Thus the generalized momentum associated with the degree of freedom, q_j, is an isolating integral, and the component of the momentum, p_j, is conserved. The variations could, in general, be functions of space or time. Then the isolating integrals resulting from the symmetry transformation would be much more complicated. However, few such isolating integrals are known aside from the ones due to the space-time symmetries.

2.3.2 Hidden Symmetries

In order for a system to be integrable, it must have as many conserved quantities as there are degrees of freedom. In general, not all of these can come from the space-time symmetries but may come from what Moser has called *hidden symmetries* [Moser 1979]. One notable example of such

a hidden symmetry occurs for the two-body Kepler problem. Because of the homogeneity of this system in time and space, the total energy and the center-of-mass momentum are conserved. In addition, the gravitational force is a central force and therefore this system exhibits isotropy in space, which means that the total angular momentum is also conserved. These space-time symmetries are sufficient to make this system integrable since they provide six conservation laws for the six degrees of freedom. However, there is still another conserved quantity, the Laplace-Runge-Lenz vector

$$\mathbf{A} = \mathbf{p} \times \mathbf{L} - \mu k \frac{\mathbf{r}}{|\mathbf{r}|} \tag{2.3.16}$$

[Moser 1970], [Abarbanel 1976], [Goldstein 1980], where $\mathbf{p}$ is the relative momentum, $\mathbf{L}$ is the total angular momentum, μ and k are as defined in Sect. 2.2, and $\mathbf{r}$ is the relative displacement of the two bodies. This additional symmetry is responsible for the fact that there is no precession of the perihelion (the point of closest approach of the two bodies) for the two-body Kepler system. This conservation law does not hold for any other central force problem.

Hidden symmetries underlie the relatively new field of soliton physics. One type of soliton, the nontopological soliton, occurs in integrable dynamical systems and is most commonly found in continuous media and on length scales where the underlying discreteness of matter plays no role. There is one mechanical system with a finite number of degrees of freedom, however, that is now known to support solitons. That is the N-body Toda lattice [Toda 1967], [Toda 1981]. The Toda lattice is a collection of equal-mass particles coupled in one dimension by exponentially varying forces. It is integrable and therefore has N isolating integrals of the motion. The Toda lattice is one of the few discrete lattices for which soliton solutions are exact. The continuum limit of the Toda lattice yields the Korteweg-de Vries equation, which is the classic equation describing nontopological solitons in continuum mechanics. The first real indication that the Toda lattice was integrable came from numerical experiments by Ford et al. [Ford et al. 1973]. This prompted theoretical work by Henon [Henon 1974] and Flaschka [Flaschka 1974], who found expressions for the N isolating integrals of the motion. The actual solution of the equations of motion was due to Date and Tanaka [Date and Tanaka 1976], although significant contributions were made by Kac and van Moerbeke [Kac and van Moerbeke 1975].

If we use techniques from soliton physics, it is fairly easy to show that the Toda lattice is integrable. Let us demonstrate this for the three-body Toda lattice. For a periodic one-dimensional lattice, the Hamiltonian can be written

$$H = \frac{p_1^2}{2} + \frac{p_2^2}{2} + \frac{p_3^2}{2} + (e^{-(q_1-q_2)} + e^{-(q_2-q_3)} + e^{-(q_3-q_1)} - 3). \tag{2.3.17}$$

This system has three degrees of freedom since the three masses move in one spatial dimension. The equations of motion are

$$\dot{p}_i = -\frac{\partial H}{\partial q_i} = (e^{-(q_i - q_{i+1})} - e^{-(q_{i-1} - q_i)}) \tag{2.3.18}$$

and

$$\dot{q}_i = \frac{\partial H}{\partial p_i} = p_i, \tag{2.3.19}$$

where $i = 1, 2, 3$, and $q_{i+3} = q_i$, $p_{i+3} = p_i$ due to the periodicity of the lattice. Following Flaschka [Flaschka 1974], let us make a noncanonical transformation to new variables $(\{a_i\}, \{b_i\})$ for $(i = 1, 2, 3)$, where

$$a_i = \frac{1}{2} e^{-\frac{1}{2}(q_i - q_{i+1})} \quad \text{and} \quad b_i = \frac{p_i}{2}. \tag{2.3.20}$$

Let us now introduce the symmetric matrix

$$\bar{A}(t) = \begin{pmatrix} b_1 & a_1 & a_3 \\ a_1 & b_2 & a_2 \\ a_3 & a_2 & b_3 \end{pmatrix} \tag{2.3.21}$$

and the antisymmetric matrix

$$\bar{B}(t) = \begin{pmatrix} 0 & a_1 & -a_3 \\ -a_1 & 0 & a_2 \\ a_3 & -a_2 & 0 \end{pmatrix}. \tag{2.3.22}$$

The equations of motion can then be written in the form

$$\frac{d\bar{A}(t)}{dt} = \bar{B}(t)\bar{A}(t) - \bar{A}(t)\bar{B}(t). \tag{2.3.23}$$

The matrices $\bar{A}(t)$ and $\bar{B}(t)$ are called Lax pairs [Lax 1968]. They are functions of the canonical coordinates, $(\{p_i, q_i\})$, and, therefore, will vary in time. The Hamiltonian, H, is related to the trace of $\bar{A}^2(t)$,

$$\operatorname{Tr} \bar{A}^2(t) = b_1^2 + b_2^2 + b_3^2 + 2(a_1^2 + a_2^2 + a_3^2) = \frac{1}{2}(H + 3). \tag{2.3.24}$$

Since this is a conservative system, $\operatorname{Tr} \bar{A}^2(t)$ is independent of time.

Toda type lattices are the only known three-body mechanical systems for which Lax pairs can be constructed. The fact that Eq. (2.3.23) holds automatically means that the three-body Toda lattice is integrable. We can see this as follows. Let us introduce yet another matrix, $\bar{O}(t)$, which is a solution of the equation

$$\frac{d\bar{O}(t)}{dt} = \bar{B}(t)\bar{O}(t). \tag{2.3.25}$$

Since $\bar{B}(t)$ is antisymmetric, $\bar{O}(t)$ is orthogonal. That is, $\bar{O}^T(t) = \bar{O}^{-1}(t)$, where $\bar{O}^T(t)$ is the transpose and $\bar{O}^{-1}(t)$ is the inverse of $\bar{O}(t)$. We also

can write

$$\frac{d\bar{O}^{-1}(t)}{dt} = -\bar{O}^{-1}(t)\bar{B}(t). \tag{2.3.26}$$

Using Eqs. (2.3.25) and (2.3.26), we can write Eq. (2.3.23) as

$$\frac{d\bar{A}(t)}{dt} = \frac{d\bar{O}(t)}{dt}\bar{\mathcal{L}}\bar{O}^{-1}(t) + \bar{O}(t)\bar{\mathcal{L}}\frac{d\bar{O}^{-1}(t)}{dt}, \tag{2.3.27}$$

where the matrix $\bar{\mathcal{L}}$ is defined as

$$\bar{\mathcal{L}} = \bar{O}^{-1}(t)\bar{A}(t)\bar{O}(t). \tag{2.3.28}$$

Note that Eqs. (2.3.27) and (2.3.28) indicate that $\bar{\mathcal{L}}$ is independent of time. $\bar{O}(t)$ may be thought of as an evolution operator that propagates $\bar{A}(t)$ in time so that $\bar{\mathcal{L}} = \bar{A}(0)$. Let us now write

$$\bar{A}(t)\bar{\phi}(t) = \lambda(t)\bar{\phi}(t), \tag{2.3.29}$$

where $\lambda(t)$ and $\bar{\phi}(t)$ are the eigenvalues and eigenvectors, respectively, of $\bar{A}(t)$. Then, from Eq. (2.3.28) we can write

$$\bar{\mathcal{L}}\bar{O}^{-1}(t)\bar{\phi}(t) = \lambda(t)\bar{O}^{-1}(t)\bar{\phi}(t). \tag{2.3.30}$$

Thus $\lambda(t)$ is an eigenvalue of $\bar{\mathcal{L}}$ and $\bar{A}(t)$ and therefore must be independent of time (i.e., $\lambda(t) = \lambda$, where λ is a constant). If we let λ_i $(i = 1, 2, 3)$ denote the three time-independent eigenvalues of the time-dependent matrix $\bar{A}(t)$, then from Eq. (2.3.24) we can write the Hamiltonian in the form

$$H = 2\sum_{i=1}^{3}\lambda_i^2 - 3. \tag{2.3.31}$$

The eigenvalues of $\bar{A}(t)$ constitute the three independent integrals of the motion for the Toda lattice.

2.3.3 Poincaré Surface of Section

How can we tell if a system is integrable or not? There is no simple way in general. For systems with two degrees of freedom, we can check numerically by constructing a Poincaré surface of section. To see how this works, let us consider a conservative system (a system with a Hamiltonian independent of time). For such systems, the energy is conserved. The Hamiltonian is then an isolating integral of the motion and can be written

$$H(p_1, p_2, q_1, q_2) = E, \tag{2.3.32}$$

where the energy, E, is constant and restricts trajectories to lie on a three-dimensional surface in the four-dimensional phase space.

¿From Eq. (2.3.32) we can write $p_2 = p_2(p_1, q_1, q_2, E)$. If the system has a second isolating integral,

$$I_2(p_1, p_2, q_1, q_2) = C_2, \tag{2.3.33}$$

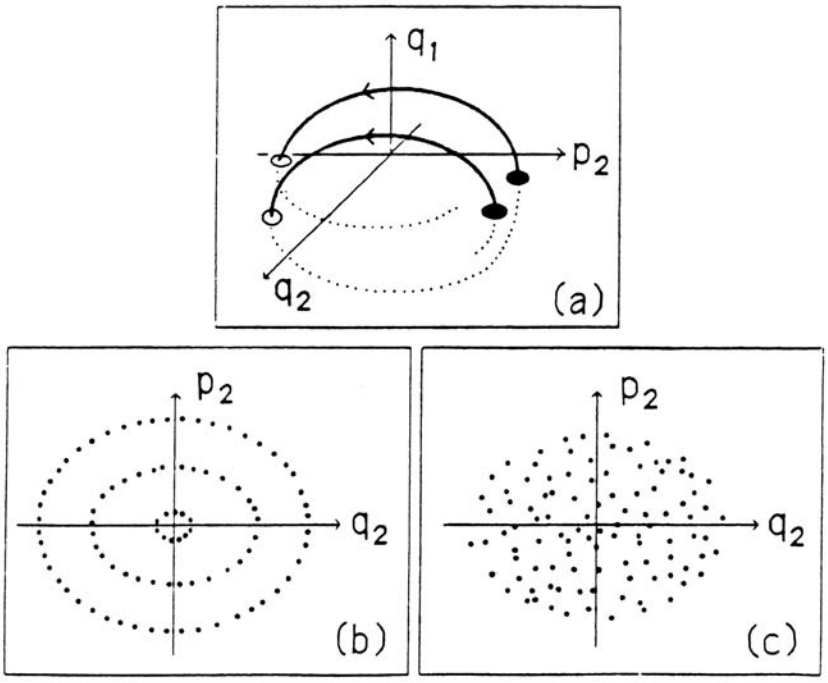

Figure 2.3.1. A Poincaré surface of section for a two degree of freedom system provides a two-dimensional map. (a) A surface of section may be obtained, for example, by plotting a point each time the trajectory passes through the plane $q_1 = 0$ with $p_1 \geq 0$. (b) If two isolating integrals exist, the trajectory will lie along one-dimensional curves in the two-dimensional surface. (c) If only one isolating integral exists (the energy), the trajectory will spread over a two-dimensional region whose extent is limited by energy conservation.

where C_2 is a constant, then it too defines a three-dimensional surface in the four-dimensional phase space. Once the initial conditions are given, E and C_2 are fixed and the trajectory is constrained to the intersection of the surfaces defined by Eqs. (2.3.32) and (2.3.33); that is, to a two-dimensional surface in the four-dimensional phase space. If we combine Eqs. (2.3.32) and (2.3.33), we can write $p_1 = p_1(q_1, q_2, E, C_2)$. If we now consider the surface $q_2 = 0$, the trajectory lies on a one-dimensional curve.

In general, if we are given the Hamiltonian, H, we do not know if an additional isolating integral, I_2, exists. We can check this numerically by solving Hamilton's equations, $\frac{dp_i}{dt} = -\frac{\partial H}{\partial q_i}$ and $\frac{dq_i}{dt} = \frac{\partial H}{\partial p_i}$, for $(i = 1, 2)$, numerically and then plotting p_2 and q_2 each time $q_1 = 0$ and $p_1 \geq 0$. (see Fig. 2.3.1.a). If the system is integrable, the trajectory will appear as a series of points (a mapping) that lie on a one-dimensional curve (see

Fig. 2.3.1.b). If the system is nonintegrable, the trajectory will appear as a scatter of points limited to a finite area due to energy conservation (see Fig. 2.3.1.c).

This method was used by Henon and Heiles [Henon and Heiles 1964] to determine if a third integral existed that constrained the motion of a star in a galaxy that had an axis of symmetry. Such a system has three degrees of freedom and two known isolating integrals of the motion, the energy and one component of the angular momentum. It was long thought that such systems do not have a third isolating integral because none had been found analytically. However, the nonexistence of a third integral implies that the dispersion of velocities of stellar objects in the direction of the galactic center is the same as that perpendicular to the galactic plane. What was observed, however, was a 2:1 ratio in these dispersions. Henon and Heiles constructed the Hamiltonian (with no known symmetries that can give rise to a third integral)

$$H = \frac{1}{2}(p_1^2 + p_2^2) + \frac{1}{2}(q_1^2 + q_2^2 + 2q_1^2 q_2 - \frac{2}{3}q_2^3) = E \tag{2.3.34}$$

to model the essential features of the problem and studied its behavior numerically. Hamilton's equations for this system are

$$\frac{dp_1}{dt} = -q_1 - 2q_1 q_2, \tag{2.3.35}$$

$$\frac{dp_2}{dt} = -q_2 - q_1^2 + q_2^2, \tag{2.3.36}$$

$$\frac{dq_i}{dt} = p_i \tag{2.3.37}$$

(for $i = 1, 2$). Note that the anharmonic terms in the potential energy give rise to nonlinear terms in the equation of motion.

A sketch of the results of Henon and Heiles is shown in Fig. 2.3.2. At low energy (see Fig. 2.3.2.a), there appears to be a third integral, at least to the accuracy of these plots. (Enlargement of the region around the hyperbolic fixed points would show a scatter of points.) As the energy is increased (this increases the effect of the nonlinear terms) (see Fig. 2.3.2.b), the third integral appears to be destroyed in the neighborhood of the hyperbolic fixed points. At still higher energies (see Fig. 2.3.2.c), the second isolating integral appears to have been totally destroyed. The scattered points in the surfaces of section for the Henon-Heiles system correspond to a single trajectory, which is chaotic. Such trajectories are chaotic in that they have *sensitive dependence on initial conditions.*

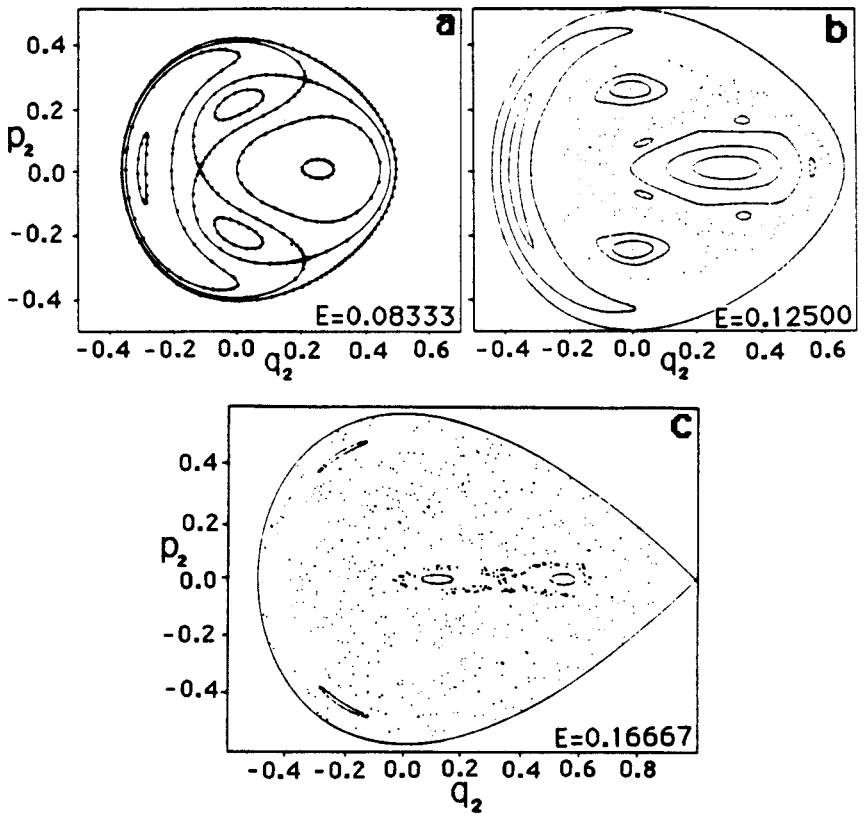

Figure 2.3.2. Poincaré surfaces of section for the Henon-Heiles system. (a) At energy $E = 0.08333$, the system appears to have two isolating integrals of the motion, at least to the scale of these plots. (b) At energy $E = 0.12500$, a chaotic trajectory appears in the neighborhood of the hyperbolic fixed points. (c) At energy $E = 0.16667$, the energy surface has become almost entirely chaotic. [Henon and Heiles 1964]

2.4 Nonlinear Resonance and Chaos

Chaotic regions occur when isolating integrals of motion are destroyed locally by nonlinear resonances. Walker and Ford [Walker and Ford 1969] show this explicitly for a simple model Hamiltonian. Let us first consider the case of a nonlinear system with two degrees of freedom and with a single resonance between these two degrees of freedom.

2.4.1 Single-Resonance Hamiltonians

In terms of action-angle variables, a general single-resonance Hamiltonian can be written

$$H = H_0(J_1, J_2) + \epsilon V_{n_1,n_2}(J_1, J_2)\cos(n_1\theta_1 - n_2\theta_2) = E, \tag{2.4.1}$$

where $(J_1, J_2, \theta_1, \theta_2)$ are action-angle variables. This system has a second isolating integral

$$I = n_2 J_1 + n_1 J_2 = C_2, \tag{2.4.2}$$

where C_2 is a constant. It is easy to see that Eq. (2.4.2) is an isolating integral. Write Hamilton's equations of motion for J_1 and J_2,

$$\frac{dJ_1}{dt} = -\frac{\partial H}{\partial \theta_1} = n_1 \epsilon V_{n_1,n_2}\sin(n_1\theta_1 - n_2\theta_2) \tag{2.4.3}$$

and

$$\frac{dJ_2}{dt} = -\frac{\partial H}{\partial \theta_2} = -n_2 \epsilon V_{n_1,n_2}\sin(n_1\theta_1 - n_2\theta_2). \tag{2.4.4}$$

Using Eqs. (2.4.3) and (2.4.4), we find that

$$\frac{dI}{dt} = 0. \tag{2.4.5}$$

The system described by the Hamiltonian in Eq. (2.4.1) contains a single (n_1, n_2) resonance. The presence of this resonance means that for certain values of J_1 and J_2 there can be a large transfer of energy between the two degrees of freedom of this system.

(2,2) Resonance

To see more clearly how a resonance works, let us consider the specific case of a (2,2) resonance. Following Walker and Ford, we write the Hamiltonian

$$H = H_0(J_1, J_2) + \alpha J_1 J_2 \cos(2\theta_1 - 2\theta_2) = E, \tag{2.4.6}$$

where

$$H_0(J_1, J_2) = J_1 + J_2 - J_1^2 - 3J_1 J_2 + J_2^2. \tag{2.4.7}$$

Equations (2.4.6) and (2.4.7) describe a nonlinear system because of the nonlinear dependence of H_0 on the action variables J_1 and J_2. The isolating integrals of motion are the Hamiltonian, H, and $I = 2J_1 + 2J_2$.

It is useful to make a transformation from action-angle variables $(J_1, J_2, \theta_1, \theta_2)$ to a new set of variables $(\mathcal{J}_1, \mathcal{J}_2, \Theta_1, \Theta_2)$ via the canonical transformation $\mathcal{J}_1 = J_1 + J_2 = I' = \frac{I}{2}$, $\mathcal{J}_2 = J_2$, $\Theta_1 = \theta_2$, and $\Theta_2 = \theta_2 - \theta_1$. The Hamiltonian then takes the form

$$\mathcal{H} = \mathcal{J}_1 - \mathcal{J}_1^2 - \mathcal{J}_1\mathcal{J}_2 + 3\mathcal{J}_2^2 + \alpha\mathcal{J}_2(\mathcal{J}_1 - \mathcal{J}_2)\cos(2\Theta_2) = E. \tag{2.4.8}$$

Since $\mathcal{H}$ is independent of Θ_1, in this new coordinate system $\mathcal{J}_1$ is constant. Hamilton's equations in this coordinate system become

$$\frac{d\mathcal{J}_1}{dt} = 0, \tag{2.4.9.a}$$

$$\frac{d\Theta_1}{dt} = 1 - 2\mathcal{J}_1 - \mathcal{J}_2 + \alpha\mathcal{J}_2\cos(2\Theta_2), \tag{2.4.9.b}$$

and

$$\frac{d\mathcal{J}_2}{dt} = 2\alpha\mathcal{J}_2\sin(2\Theta_2)(I' - \mathcal{J}_2), \tag{2.4.10.a}$$

$$\frac{d\Theta_2}{dt} = -I' + 6\mathcal{J}_2 + \alpha\cos(2\Theta_2)(I' - 2\mathcal{J}_2). \tag{2.4.10.b}$$

Since $\mathcal{J}_1$ is constant, Eqs. (2.4.10) can be solved first for $\mathcal{J}_2(t)$ and $\Theta_2(t)$ and then substituted into Eq. (2.4.9.b) to obtain $\Theta_1(t)$.

Let us now find the fixed points of these equations. The fixed points are points for which $\frac{d\mathcal{J}_2}{dt} = 0$ and $\frac{d\Theta_2}{dt} = 0$. Fixed points occur when $\Theta_2 = \frac{n\pi}{2}$ and $\mathcal{J}_2 = \mathcal{J}_o$, where $\mathcal{J}_o$ is a solution of the equation

$$-I' + 6\mathcal{J}_o + \alpha\cos(n\pi)(I' - 2\mathcal{J}_o) = 0. \tag{2.4.11}$$

Note that for $\alpha \ll 1$, $\mathcal{J}_o \approx \frac{I'}{6}$.

The nature of the fixed points can be determined by linearizing the equations of motion about points $(\mathcal{J}_2 = \mathcal{J}_o, \Theta_2 = \frac{n\pi}{2})$. We let $\mathcal{J}_2(t) = \mathcal{J}_o + \Delta\mathcal{J}(t)$ and $\Theta_2(t) = \frac{n\pi}{2} + \Delta\Theta(t)$ and linearize in $\Delta\mathcal{J}(t)$ and $\Delta\Theta(t)$. We find

$$\frac{d}{dt}\begin{pmatrix} \Delta\mathcal{J}(t) \\ \Delta\Theta(t) \end{pmatrix} = \begin{pmatrix} 0 & 4\alpha\cos(n\pi)\mathcal{J}_o(I' - \mathcal{J}_o) \\ (6 - 2\alpha\cos(n\pi)) & 0 \end{pmatrix} \times \begin{pmatrix} \Delta\mathcal{J}(t) \\ \Delta\Theta(t) \end{pmatrix}. \tag{2.4.12}$$

The solution $\binom{\Delta\mathcal{J}(t)}{\Delta\Theta(t)}$ to Eq. (2.4.12) determines the manner in which trajectories flow *in the neighborhood of the fixed points*. For $\alpha \ll 1$ (and therefore $\mathcal{J}_o \approx \frac{I'}{6}$), these equations reduce to

$$\frac{d}{dt}\begin{pmatrix} \Delta\mathcal{J}(t) \\ \Delta\Theta(t) \end{pmatrix} \approx \begin{pmatrix} 0 & \frac{20\alpha I'^2}{36}\cos(n\pi) \\ 6 & 0 \end{pmatrix}\begin{pmatrix} \Delta\mathcal{J}(t) \\ \Delta\Theta(t) \end{pmatrix}. \tag{2.4.13}$$

Let us assume that Eq. (2.4.13) has a solution of the form

$$\begin{pmatrix} \Delta\mathcal{J}(t) \\ \Delta\Theta(t) \end{pmatrix} = e^{\lambda t} \begin{pmatrix} A_{\mathcal{J}} \\ A_{\Theta} \end{pmatrix}, \tag{2.4.14}$$

where $A_{\mathcal{J}}$ and A_{Θ} are independent of time. Then we can solve the resulting eigenvalue equation

$$\lambda \begin{pmatrix} A_{\mathcal{J}} \\ A_{\Theta} \end{pmatrix} = \begin{pmatrix} 0 & \frac{20\alpha I'^2}{36}\cos(n\pi) \\ 6 & 0 \end{pmatrix} \begin{pmatrix} A_{\mathcal{J}} \\ A_{\Theta} \end{pmatrix}$$

for both λ and $\begin{pmatrix} A_{\mathcal{J}} \\ A_{\Theta} \end{pmatrix}$. The eigenvalues are given by

$$\lambda_{\pm} = \pm \left(\frac{20\alpha I'^2 \cos(n\pi)}{6} \right)^{\frac{1}{2}},$$

and the solution to Eq. (2.4.13) can be written

$$\begin{pmatrix} \Delta\mathcal{J}(t) \\ \Delta\Theta(t) \end{pmatrix} = e^{\lambda_+ t}\, A_+ \begin{pmatrix} \frac{b}{\lambda_+} \\ 1 \end{pmatrix} + e^{\lambda_- t}\, A_- \begin{pmatrix} \frac{b}{\lambda_-} \\ 1 \end{pmatrix}, \tag{2.4.15}$$

where $b = \frac{20\alpha I'^2}{36}$, and A_+ and A_- are determined by the initial conditions. For n even, λ is real and the solutions contain exponentially growing and decreasing components, while for n odd, λ is pure imaginary and the solutions are oscillatory. For n even, the fixed points are hyperbolic (trajectories approach or recede from the fixed point exponentially), while for n odd, the fixed points are elliptic (trajectories oscillate about the fixed point).

For *very small* α, the fixed points occur for $\mathcal{J}_2 = \mathcal{J}_o \approx \frac{I'}{6}$ and therefore for $J_1 \approx \frac{5I'}{6}$ and $J_2 \approx \frac{I'}{6}$. We can also find the range of energies for which these fixed points exist. Plugging $J_1 = 5J_2$ into Eq. (2.4.6), we find $J_1^2 - \frac{10J_1}{13} + \frac{25E}{39} = 0$ or $J_1 = \frac{5}{13}(1 \pm (1 - \frac{13E}{3})^{\frac{1}{2}}) = 5J_2$. Thus, the fixed points only exist for $E < \frac{3}{13}$ for very small α. For $E > \frac{3}{13}$, J_1 is no longer real.

A plot of some of the trajectories on the energy surface, $E = 0.18$, for coupling constant $\alpha = 0.1$, is given in Fig. 2.4.1. In this plot, we have transformed from polar coordinates $(\mathcal{J}_2, \Theta_2)$ to Cartesian coordinates (p, q) via the canonical transformation $p = -(2\mathcal{J}_2)^{\frac{1}{2}} \sin(\Theta_2)$ and $q = (2\mathcal{J}_2)^{\frac{1}{2}} \cos(\Theta_2)$. The elliptic and hyperbolic fixed points and the separatrix associated with them can be seen clearly. The region inside and in the immediate neighborhood outside the separatrix is called the (2,2) nonlinear resonance zone. We see that large changes in the action, $\mathcal{J}_2$, occur in this region of the phase space, indicating that a strong exchange of energy is occurring between the modes of the system.

Let us now attempt to compute these level curves using perturbation theory as discussed earlier. We go from action-angle variables $(J_1, J_2, \theta_1, \theta_2)$

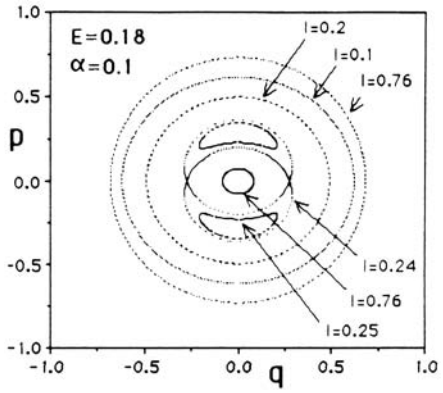

Figure 2.4.1. Phase space trajectories for the (2,2) resonance Hamiltonian in Eq. (2.4.8) ($p = -(2\mathcal{J}_2)^{\frac{1}{2}}\sin(\Theta_2)$ and $q = (2\mathcal{J}_2)^{\frac{1}{2}}\cos(\Theta_2)$). For all curves, $E = 0.18$ and $\alpha = 0.1$. The curves consist of discrete points because we have plotted points along the trajectories at discrete times.

to new variables $(\mathcal{I}_1, \mathcal{I}_2, \phi_1, \phi_2)$ via a canonical transformation given by the generating function

$$G(\mathcal{I}_1, \mathcal{I}_2, \phi_1, \phi_2) = \mathcal{I}_1\theta_1 + \mathcal{I}_2\theta_2 + \alpha g_{2,2}(\mathcal{I}_1, \mathcal{I}_2)\sin(2\theta_1 - 2\theta_2). \quad (2.4.16)$$

Following the procedure outlined in Sect. 2.2, we find that $g_{2,2} = \frac{-\mathcal{I}_1\mathcal{I}_2}{(2\omega_1 - 2\omega_2)}$, where $\omega_1 = 1 - 2\mathcal{I}_1 - 3\mathcal{I}_2$ and $\omega_2 = 1 - 3\mathcal{I}_1 + 2\mathcal{I}_2$. The Hamiltonian to order α^2 is $H = H_o(\mathcal{I}_1, \mathcal{I}_2) + O(\alpha^2)$ and the action variables (neglecting terms of order α^2) are

$$J_1(t) = \mathcal{I}_1 - \frac{2\alpha\mathcal{I}_1\mathcal{I}_2\cos(2\omega_1 t - 2\omega_2 t)}{(2\omega_1 - 2\omega_2)} \quad (2.4.17)$$

and

$$J_2(t) = \mathcal{I}_2 + \frac{2\alpha\mathcal{I}_1\mathcal{I}_2\cos(2\omega_1 t - 2\omega_2 t)}{(2\omega_1 - 2\omega_2)}. \quad (2.4.18)$$

In order for these equations to have meaning, the following condition must hold:

$$|2\omega_1 - 2\omega_2| = |2\mathcal{I}_1 - 10\mathcal{I}_2| \gg 2\alpha\mathcal{I}_1\mathcal{I}_2.$$

However, near a resonance, $\mathcal{I}_1 \approx 5\mathcal{I}_2$. Therefore this condition breaks down in the neighborhood of a resonance zone. Actually this is to be expected since the resonance introduces a topological change in the flow pattern in the phase space.

(2,3) Resonance

Walker and Ford also studied a (2,3) resonance with Hamiltonian

$$H = H_o(J_1, J_2) + \beta J_1 J_2^{\frac{3}{2}} \cos(2\theta_1 - 3\theta_2) = E. \tag{2.4.19}$$

This again is integrable and has two isolating integrals of the motion, the Hamiltonian, H, and

$$I = 3J_1 + 2J_2 = C_3. \tag{2.4.20}$$

We can again make a canonical transformation, $J_1 = \mathcal{J}_1 - \frac{2}{3}\mathcal{J}_2, J_2 = \mathcal{J}_2, \theta_1 = \Theta_1, \theta_2 = \Theta_2 + \frac{2}{3}\Theta_1$ (note that $I = 3\mathcal{J}_1$). The Hamiltonian then takes the form

$$\mathcal{H} = \mathcal{J}_1 - \mathcal{J}_1^2 + \frac{\mathcal{J}_2}{3} - \frac{5\mathcal{J}_1\mathcal{J}_2}{3} + \frac{23}{9}\mathcal{J}_2^2 + \frac{\beta}{3}\mathcal{J}_2^{\frac{3}{2}}(3\mathcal{J}_1 - 2\mathcal{J}_2)\cos(3\Theta_2) = E \tag{2.4.21}$$

and the coordinate $\mathcal{J}_1$ is a constant of the motion since $\mathcal{H}$ is independent of Θ_1. The equations of motion for $\mathcal{J}_2$ and Θ_2 are

$$\frac{d\mathcal{J}_2}{dt} = \beta\mathcal{J}_2^{\frac{3}{2}}(3\mathcal{J}_1 - 2\mathcal{J}_2)\sin(3\Theta_2) \tag{2.4.22}$$

and

$$\frac{d\Theta_2}{dt} = \frac{1}{3} - \frac{5\mathcal{J}_1}{3} + \frac{46\mathcal{J}_2}{9} + \beta\mathcal{J}_2^{\frac{1}{2}}\left(\frac{3}{2}\mathcal{J}_1 - \frac{5}{3}\mathcal{J}_2\right)\cos(3\Theta_2). \tag{2.4.23}$$

It is easy to see that the fixed points occur for $\Theta_2 = \frac{n\pi}{3}$ and $\mathcal{J}_2 = \mathcal{J}_o$ where $\mathcal{J}_o$ satisfies the equation

$$\frac{1}{3} - \frac{5I}{9} + \frac{46\mathcal{J}_o}{9} + \beta\mathcal{J}_o^{\frac{1}{2}}\left(\frac{I}{2} - \frac{5}{3}\mathcal{J}_o\right)\cos(n\pi) = 0. \tag{2.4.24}$$

If we again linearize the equations of motion about these fixed points and determine the form of the flow in their neighborhood as we did below Eq. (2.4.11), we find that for even n ($n = 0, 2, 4$) the fixed points are hyperbolic while for odd n ($n = 1, 3, 5$) the fixed points are elliptic. These fixed points are clearly seen in the plot of the phase space trajectories for the (2,3) resonance system given in Fig. 2.4.2. In Fig. 2.4.2 all curves have energy $E = 0.18$ and coupling constant $\beta = 0.1$. The separatrix of the (2,3) resonance zone is clearly seen, as are the three hyperbolic and elliptic fixed points.

2.4.2 Two-Resonance Hamiltonian

The two single-resonance systems described above are integrable. Any systems containing two or more resonances are nonintegrable because a second isolating integral of the motion cannot be found. Therefore systems with two or more resonances can undergo a transition to chaos as parameters

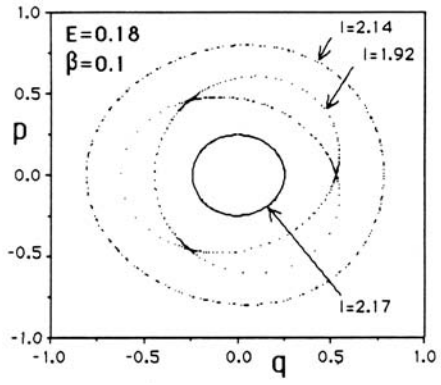

Figure 2.4.2. A plot of some phase space trajectories obtained for the (2,3) resonance Hamiltonian in Eq. (2.4.19). All curves have energy $E = 0.18$ and coupling constant $\beta = 0.1$ but have different values of the constant of motion, I. The three hyperbolic and three elliptic fixed points as well as the separatrix of the (2,3) resonance are clearly seen. The curves consist of discrete points because we plot points along the trajectories at discrete times. We have set $p = -(2\mathcal{J}_2)^{\frac{1}{2}} \sin(\Theta_2)$ and $q = (2\mathcal{J}_2)^{\frac{1}{2}} \cos(\Theta_2)$.

of the system are varied. Walker and Ford show this for the Hamiltonian with two primary resonances,

$$H = H_o(J_1, J_2) + \alpha J_1 J_2 \cos(2\theta_1 - 2\theta_2) + \beta J_1 J_2^{\frac{3}{2}} \cos(2\theta_1 - 3\theta_2) = E. \tag{2.4.25}$$

The surface of section for this Hamiltonian is shown in Fig. 2.4.3.

Hamilton's equations for the two-resonance system can be written

$$\frac{dJ_1}{dt} = -\frac{\partial H}{\partial \theta_1} = 2\alpha J_1 J_2 \sin(2\theta_1 - 2\theta_2) + 2\beta J_1 J_2^{\frac{3}{2}} \sin(2\theta_1 - 3\theta_2), \tag{2.4.26}$$

$$\frac{dJ_2}{dt} = -\frac{\partial H}{\partial \theta_2} = -2\alpha J_1 J_2 \sin(2\theta_1 - 2\theta_2) - 3\beta J_1 J_2^{\frac{3}{2}} \sin(2\theta_1 - 3\theta_2), \tag{2.4.27}$$

$$\frac{d\theta_1}{dt} = \frac{\partial H}{\partial J_1} = 1 - 2J_1 - 3J_2 + \alpha J_2 \cos(2\theta_1 - 2\theta_2) + \beta J_2^{\frac{3}{2}} \cos(2\theta_1 - 3\theta_2), \tag{2.4.28}$$

$$\frac{d\theta_2}{dt} = \frac{\partial H}{\partial J_2} = 1 - 3J_1 + 2J_2 + \alpha J_1 \cos(2\theta_1 - 2\theta_2) + \frac{3}{2}\beta J_1 J_2^{\frac{1}{2}} \cos(2\theta_1 - 3\theta_2). \tag{2.4.29}$$

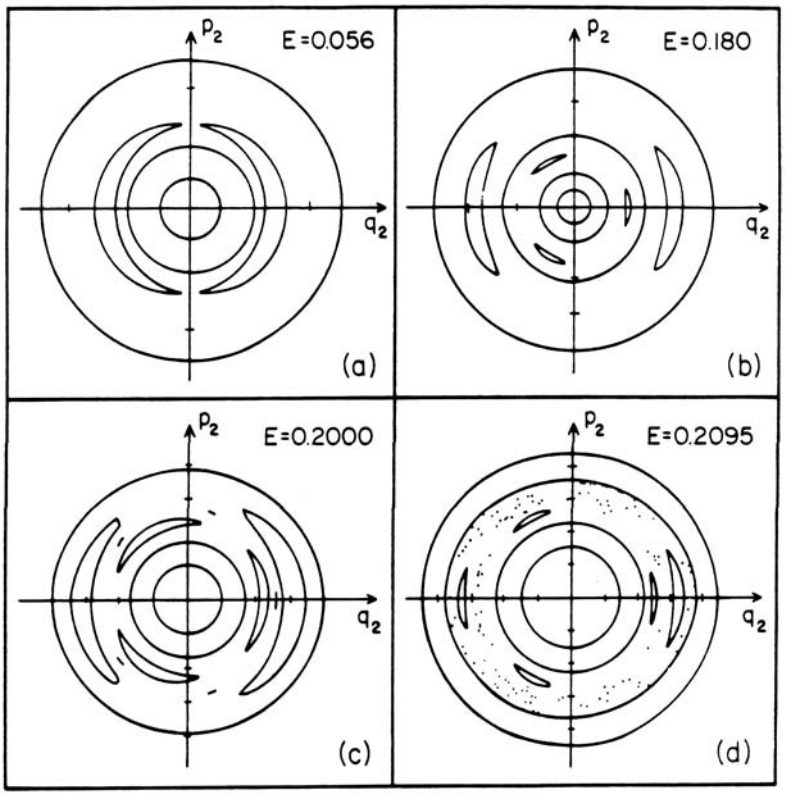

Figure 2.4.3. Poincaré surfaces of section for the double-resonance Hamiltonian in Eq. (2.4.25) with $p_2 = -(2J_2)^{\frac{1}{2}} \sin(\theta_2)$ and $q_2 = (2J_2)^{\frac{1}{2}} \cos(\theta_2)$ and coupling constants $\alpha = \beta = 0.02$. (a) At energy $E = 0.056$, only the (2,2) resonance exists. (b) At energy $E = 0.180$, the (2,3) resonance has emerged from the origin but is well-separated from the (2,2) resonance. (c) At energy $E = 0.2000$, the two primary resonances have grown in size but remain separated. The chain of five islands is a higher-order resonance. (d) At energy $E = 0.2095$, resonance overlap has occurred and chaos can be seen in the overlap region. [Walker and Ford 1969]

Walker and Ford construct a Poincaré surface of section by solving the equations of motion (2.4.26)−(2.4.29) numerically and plotting (J_2, θ_2) each time $\theta_1 = \frac{3\pi}{2}$. (If $p_i = -(2J_i)^{\frac{1}{2}} \sin(\theta_i)$ and $q_i = (2J_i)^{\frac{1}{2}} \cos(\theta_i)$, the surface of section is similar to that of Henon and Heiles, who plot a point (p_2, q_2) each time $q_1 = 0$ and $p_1 > 0$.) A sketch of the Poincaré surface of section for several energies is shown in Fig. 2.4.3. In all cases shown in this figure, the coupling constants are $\alpha = \beta = 0.02$, a value much smaller than those used in Figs. 2.4.1 and 2.4.2. The (2,2) resonance is present for all energies $E \leq \frac{3}{13}$. However, the (2,3) resonance first emerges from the origin for energy $E \approx 0.16$. For energies $E = 0.056$ (Fig. 2.4.3.a), only the (2,2) resonance exists. For $E = 0.180$ (Fig. 2.4.3.b), both resonances are present but well-separated in the phase space. As the energy is raised, the resonances occupy larger regions of the phase space. Finally, for $E = 0.2095$ (Fig. 2.4.3.d), the resonances have overlapped and a chaotic trajectory is found.

2.5 KAM Theory

As we have seen in Sect. 2.2, conventional perturbation theory diverges in regions containing resonance zones because of small denominators arising from the resonances. However, Kolmogorov [Kolmogorov 1954] found a way to construct a perturbation theory that was rapidly convergent and applicable to nonresonant tori. Kolmogorov's ideas were made rigorous by Arnol'd [Arnol'd 1963] and by Moser [Moser 1962]. The nonresonant tori that have not been destroyed by resonances are called KAM tori or KAM surfaces (after Kolmogorov, Arnol'd, and Moser). Examples of KAM tori can be found in Figs. 2.3.2 and 2.4.3, and many more will be seen throughout this book.

The KAM theory applies to systems with N degrees of freedom whose motion is governed by a Hamiltonian of the form

$$H(J_1, \ldots, J_N, \theta_1, \ldots, \theta_N) = H_0(J_1, \ldots, J_N) + \epsilon V(J_1, \ldots, J_N, \theta_1, \ldots, \theta_N), \tag{2.5.1}$$

where H_0 is integrable, ϵ is a small parameter, and the potential energy, $V(J_1, \ldots, J_N, \theta_1, \ldots, \theta_N)$, can be written in the form

$$V = \sum_{n_1} \cdots \sum_{n_N} V_{n_1, \ldots n_N}(J_1, \ldots, J_N)\ e^{i(n_1\theta_1 + \cdots + n_N\theta_N)}, \tag{2.5.2}$$

where n_i $(i = 1, \ldots, N)$ ranges over all integers. (Note that if $V(J_1, \ldots, J_N, \theta_1, \ldots, \theta_N)$ is a smooth function of angles, $\{\theta_i\}$, the Fourier coefficients, $V_{n_1, \ldots n_N}$, will decrease fairly rapidly with increasing $\{n_i\}$.) A further requirement that is necessary for the proof of the KAM theorem is that the

determinant of the matrix formed by the quantities $\frac{\partial^2 H_0}{\partial J_i \partial J_j}$ (the Hessian of H_0) must be nonzero.

The Hamiltonian defined in Eq. (2.5.1) describes a system with a dense set of resonances in phase space. KAM showed that for such systems, the volume of phase space occupied by resonances goes to zero as $\epsilon \to 0$. The idea behind this can be illustrated by a simple example. Consider the unit line (a continuous line ranging from zero to one). This line contains an infinite number of rational fractions. However, the rational fractions form a set of measure zero. Now exclude a region

$$\left(\frac{m}{n} - \frac{\epsilon}{n^3}\right) \leq \frac{m}{n} \leq \left(\frac{m}{n} + \frac{\epsilon}{n^3}\right)$$

about each rational fraction. This mimics resonances that have finite width, $\frac{2\epsilon}{n^3}$ for example, and are located in regions of the phase space for which the ratio of frequencies associated with the various degrees of freedom is a rational fraction. The total length of the line that is excluded is

$$\sum_{n=1}^{\infty} \sum_{m=1}^{n} \left(\frac{2\epsilon}{n^3}\right) = 2\epsilon \sum_{n=1}^{\infty} \left(\frac{1}{n^2}\right) = \frac{\epsilon \pi^2}{3} \to 0 \quad \text{as} \quad \epsilon \to 0.$$

Thus, for very small ϵ, only a small fraction of the total volume of phase space contains resonance zones. But they exist on all scales.

We do not have space here to prove the KAM theorem (for this, one should go to the references cited above), but we will try to give the flavor of it. Let us illustrate the approach for the case of a system with two degrees of freedom. We follow the discussion by Barrar [Barrar 1970], which most closely follows Kolmogorov's original approach.

• *The KAM theorem (for $N = 2$)*

Consider a system described by the Hamiltonian

$$H(J_1, J_2, \theta_1, \theta_2) = H_o(J_1, J_2) + \epsilon \sum_{n_1=-\infty}^{\infty}{}' \sum_{n_2=-\infty}^{\infty}{}' V_{n_1,n_2}(J_1, J_2) e^{i(n_1\theta_1 + n_2\theta_2)}, \tag{2.5.3}$$

where ϵ is a *small* parameter and H_0 has nonzero Hessian. The prime on the summations indicates that we exclude the term $n_1 = n_2 = 0$ since it can be included in H_0. We shall assume that H is an analytic function of all variables and is a periodic function of angles θ_1 and θ_2. On a torus $(J_1 = J_1^o, J_2 = J_2^o)$ such that the frequencies $\omega_i = (\frac{\partial H_o}{\partial J_j})_o = \omega_i(J_1^o, J_2^o)$ satisfy the conditions

$$|n_1\omega_1 + n_2\omega_2| \geq \frac{K}{||n||^\alpha},$$

where $||n|| = |n_1| + |n_2| > 0$, $\alpha \geq 2$, and K is a constant, a perturbation theory will converge. •

The proof of the KAM theorem proceeds as follows (see [Kolmogorov 1954] and [Barrar 1970] for details). Let us move the origin of coordinates to (J_1^o, J_2^o) via a canonical transformation, $J_i - J_i^o = p_i$ and $\theta_i = \phi_i$. The Hamiltonian then can be written in the form

$$H = C^0 + \sum_{i=1}^{2} \omega_i p_i + \epsilon A^{(0)}(\phi_1, \phi_2) + \epsilon \sum_{i=1}^{2} B_i^{(0)}(\phi_1, \phi_2) p_i + \sum_{i=1}^{2} \sum_{j=1}^{2} C_{i,j}^{(0)}(\phi_1, \phi_2) p_i p_j + D^{(0)}(p_1, p_2, \phi_1, \phi_2), \tag{2.5.4}$$

where $C^{(0)}$ is a constant and $D^{(0)}(p_1, p_2, \phi_1, \phi_2)$ is a function whose lowest-order dependence on p_i is p_i^3. Let us now introduce a generating function that takes us from coordinates $(p_1, p_2, \phi_1, \phi_2)$ to a new set of canonical coordinates $(P_1^{(1)}, P_2^{(1)}, \Phi_1^{(1)}, \Phi_2^{(1)})$. We write the generating function in the form

$$S(P_1^{(1)}, P_2^{(1)}, \phi_1, \phi_2) = \sum_{i=1}^{2} (P_i^{(1)} + \epsilon \xi_i)\phi_i + \epsilon X(\phi_1, \phi_2) + \epsilon \sum_{i=1}^{2} P_i^{(1)} Y_i(\phi_1, \phi_2), \tag{2.5.5}$$

where ξ_i are constants and X and Y_i are functions to be determined. Then

$$p_i = \frac{\partial S}{\partial \phi_i} = (P_i^{(1)} + \epsilon \xi_i) + \epsilon \frac{\partial X}{\partial \phi_i} + \epsilon \sum_{j=1}^{2} P_j^{(1)} \frac{\partial Y_j}{\partial \phi_i} \tag{2.5.6}$$

and

$$\Phi_i^{(1)} = \frac{\partial S}{\partial P_i^{(1)}} = \phi_i + \epsilon Y_i(\phi_1, \phi_2). \tag{2.5.7}$$

We can use Eqs. (2.5.6) and (2.5.7) to write the Hamiltonian in terms of new coordinates, $(P_1^{(1)}, P_2^{(1)}, \Phi_1^{(1)}, \Phi_2^{(1)})$. The idea of Kolmogorov was to choose the quantities X,Y_i and ξ_i so that they cancel $A^{(0)}$ and $B_i^{(0)}$ from the resulting Hamiltonian. (Most of Barrar's paper is devoted to showing that this can be done.) Then, in terms of the new canonical coordinates, $(P_1^{(1)}, P_2^{(1)}, \Phi_1^{(1)}, \Phi_2^{(1)})$, the Hamiltonian becomes

$$H^{(1)} = C^{(1)} + \sum_{i=1}^{2} \omega_i P_i^{(1)} + \epsilon^2 A^{(1)}(\Phi_1^{(1)}, \Phi_2^{(1)}) + \epsilon^2 \sum_{i=1}^{2} B_i^{(1)}(\Phi_1^{(1)}, \Phi_2^{(1)}) P_i^{(1)} + \sum_{i=1}^{2} \sum_{j=1}^{2} C_{i,j}^{(1)}(\Phi_1^{(1)}, \Phi_2^{(1)}) P_i^{(1)} P_j^{(1)} + D^{(1)}(P_1^{(1)}, P_2^{(1)}, \Phi_1^{(1)}, \Phi_2^{(1)}). \tag{2.5.8}$$

This process can be repeated. In the next step, the Hamiltonian becomes

$$H^{(2)} = C^{(2)} + \sum_{i=1}^{2} \omega_i P_i^{(2)} + \epsilon^4 A^{(2)}(\Phi_1^{(2)}, \Phi_2^{(2)}) + \epsilon^4 \sum_{i=1}^{2} B_i^{(2)}(\Phi_1^{(2)}, \Phi_2^{(2)}) P_i^{(2)} + \sum_{i=1}^{2}\sum_{j=1}^{2} C_{i,j}^{(2)}(\Phi_1^{(2)}, \Phi_2^{(2)}) P_i^{(2)} P_j^{(2)} + D^{(2)}(P_1^{(2)}, P_2^{(2)}, \Phi_1^{(2)}, \Phi_2^{(2)}). \tag{2.5.9}$$

The sequence of Hamiltonians obtained by this procedure converges very rapidly to the form

$$H^{(\infty)} = C^{(\infty)} + \sum_{i=1}^{2} \omega_i P_i^{(\infty)} + \sum_{i=1}^{2}\sum_{j=1}^{2} C_{i,j}^{\infty}(\Phi_1^{(\infty)}, \Phi_2^{(\infty)}) P_i^{(\infty)} P_j^{(\infty)} + D^{\infty}(P_1^{(\infty)}, P_2^{(\infty)}, \Phi_1^{(\infty)}, \Phi_2^{(\infty)}). \tag{2.5.10}$$

In terms of the coordinates $(P_1^{(\infty)}, P_2^{(\infty)}, \Phi_1^{(\infty)}, \Phi_2^{(\infty)})$, Hamilton's equations take the form

$$\frac{dP_k^{(\infty)}}{dt} = -\frac{\partial H^{(\infty)}}{\partial \Phi_k^{(\infty)}} = \sum_{i=1}^{2}\sum_{j=1}^{2} P_i^{(\infty)} P_j^{(\infty)} \frac{\partial C_{i,j}^{(\infty)}}{\partial \Phi_k^{(\infty)}} + O((P^{(\infty)})^3) \tag{2.5.11}$$

and

$$\frac{d\Phi_k^{(\infty)}}{dt} = \frac{\partial H^{(\infty)}}{\partial P_k^{(\infty)}} = \omega_k + O((P^{(\infty)})^3) \tag{2.5.12}$$

for $(k = 1, 2)$. These equations have solutions $P_i^{(\infty)} = 0$ and $\Phi_i^{(\infty)} = \omega_i t + C_i$ for $(i = 1, 2)$, where C_i is a constant.

Thus, a rapidly convergent procedure has been found to obtain solutions to the equations of motion at least on KAM tori sufficiently far from resonances.

2.6 The Definition of Chaos

.

The flow of trajectories in a given region of phase space is said to be chaotic if it has positive KS metric entropy (KS stands for Krylov, Kolmogorov, and Sinai) [Kolmogorov 1958, 1959], [Sinai 1963a], [Arnol'd and Avez 1968], [Ornstein 1974], [Chirikov 1979], [Lichtenberg and Lieberman 1983]. *Such flows are called K-flows.* The KS entropy is a measure of the degree of hyperbolic instability in the relative motion of trajectories in phase space. As we saw in Sect. 2.4, in the neighborhood of fixed points, we can determine the nature of the flow by linearizing the equations of motion about the fixed point. In the neighborhood of hyperbolic fixed points,

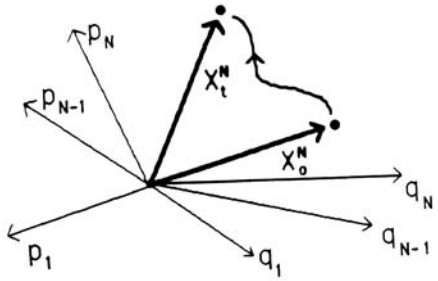

Figure 2.6.1. The $2N$-dimensional vector, $\mathbf{X}_t^N$, evolves according to Hamilton's equations and describes the evolution of the state of the system in phase space.

trajectories on the eigenvectors approach (depart) the fixed point in an exponentially decreasing (increasing) manner. Trajectories in the neighborhood of the fixed point, but not on the eigenvectors, contain both types of motion. There are as many sets of eigenvectors in the neighborhood of a hyperbolic fixed point as there are degrees of freedom. Along each eigenvector, the rate of approach or departure is determined by a single eigenvalue of the transition matrix (the matrix that governs the evolution in the neighborhood of the fixed point) for the linearized problem.

2.6.1 Lyapounov Exponent

Oseledec [Oseledec 1968] was the first to show that a procedure analogous to that used to study exponential divergence of flow in the neighborhood of hyperbolic fixed points could be used to study the nature of the flow in the neighborhood of a moving point in phase space. To see how this works, consider a system with N degrees of freedom ($2N$-dimensional phase space). We shall denote the $2N$-dimensional vector describing the state of the system at time t by $\mathbf{X}_t^N = \mathbf{X}^N(p_1(t), \ldots, p_N(t); q_1(t), \ldots, q_N(t))$ (see Fig. 2.6.1). This vector evolves according to Hamilton's equations. Let us now consider two neighboring points in phase space, $\mathbf{X}_t^N$ and $\mathbf{Y}_t^N = \mathbf{X}_t^N + \Delta\mathbf{X}_t^N$. By solving Hamilton's equations for our system, we can determine how the displacement, $\Delta\mathbf{X}_t^N$, evolves in time. We define the magnitude of the displacement, $\Delta\mathbf{X}_t^N$, to be

$$d_t(\mathbf{X}_o^N, \mathbf{Y}_o^N) = |\Delta\mathbf{X}_t^N| = (\Delta\mathbf{X}_t^N \cdot \Delta\mathbf{X}_t^N)^{\frac{1}{2}}, \tag{2.6.1}$$

where $\mathbf{X}_o^N$ and $\mathbf{Y}_o^N$ are the initial values of $\mathbf{X}_t^N$ and $\mathbf{Y}_t^N$. The rate of exponential growth (or decrease) of $d_t(\mathbf{X}_o^N, \mathbf{Y}_o^N)$ is given by

$$\lambda(\mathbf{X}_o^N, \mathbf{Y}_o^N) = \lim_{t\to\infty} \frac{1}{t} \ln\left(\frac{d_t(\mathbf{X}_o^N, \mathbf{Y}_o^N)}{d_o(\mathbf{X}_o^N, \mathbf{Y}_o^N)}\right). \tag{2.6.2}$$

$\lambda(\mathbf{X}_o^N, \mathbf{Y}_o^N)$ is called the *Lyapounov exponent*.

There are $2N$ orthogonal directions in a $2N$-dimensional phase space and therefore $2N$ independent Lyapounov exponents. We let the set $\{\mathbf{e}_i\}$

denote the $2N$ unit vectors associated with these $2N$ orthogonal directions, where the unit vector, $\mathbf{e}_i$, denotes the direction in which the separation of neighboring trajectories is characterized by λ_i. Then, in general, we can write $\Delta\mathbf{X}_t = \sum_{i=1}^{2N} C_i(t)\mathbf{e}_i$, where the coefficient, $C_i(t)$, denotes the component of $\Delta\mathbf{X}_t$ in the direction $\mathbf{e}_i$. The Lyapounov exponent associated with the direction $\mathbf{e}_i$ is given by

$$\lambda_i = \lambda(\mathbf{X}_o^N, \mathbf{e}_i) = \lim_{t\to\infty} \frac{1}{t} \ln\left(\frac{d_t(\mathbf{X}_o^N, \mathbf{e}_i)}{d_o(\mathbf{X}_o^N, \mathbf{e}_i)}\right). \tag{2.6.3}$$

The notation $d_t(\mathbf{X}_o^N, \mathbf{e}_i)$ indicates that we choose a neighboring point, $\mathbf{Y}_o^N$, so that it deviates from $\mathbf{X}_o^N$ only in the direction $\mathbf{e}_i$ in phase space.

In [Benettin and Strelcyn 1978] it is shown that, for Hamiltonian flows, the exponents satisfy the relation

$$\lambda_i = -\lambda_{2N-i+1}. \tag{2.6.4}$$

On the energy surface, there are $2N-1$ exponents. One of them is zero (the one associated with motion along the direction of the flow). We can now order the exponents in order of increasing value. If we relabel the indices in Eq. (2.6.4), we can write

$$-\lambda_{N-1} \leq \ldots \leq -\lambda_1 \leq 0 \leq \lambda_1 \leq \ldots \leq \lambda_{N-1}.$$

If $\Delta\mathbf{X}_t$ is chosen arbitrarily, it should contain some contribution from all spatial directions. Then we will find $\lambda(\mathbf{X}_o^N, \mathbf{Y}_o^N) = \lambda_{N-1}$. A numerical method for computing all $2N$ of the Lyapounov exponents in an N degree of freedom system can be found in [Benettin et al. 1979].

Benettin et al. [Benettin et al. 1976] have computed λ_{N-1} for the Henon-Heiles system. For bounded systems, the quantity defined in Eq. (2.6.2) can be expected to saturate after a finite time. Thus a slightly different procedure is used to obtain the exponents. One essentially computes a sequence of distances each of which is obtained after a finite length of time, τ, in the following way. Let $\mathbf{X}_{o,n-1}$ ($\mathbf{X}_{\tau,n-1}$) denote the position of our reference trajectory at the beginning (end) of the nth time step, τ.

Let $\mathbf{X}_{o,o}$ and $\mathbf{Y}_{o,o}$ denote the positions of neighboring trajectories at the initial time. Initially, the distance between them is $d_o = |\mathbf{Y}_{o,o} - \mathbf{X}_{o,o}|$. At the end of the first time step, their distance is $d_1 = |\mathbf{Y}_{\tau,o} - \mathbf{X}_{\tau,o}|$. Now begin the second time step. We relabel the position of our reference trajectory, $\mathbf{X}_{o,1} = \mathbf{X}_{\tau,o}$, and choose a new neighboring vector, $\mathbf{Y}_{o,1}$, so that the vector $(\mathbf{Y}_{o,1} - \mathbf{X}_{o,1})$ is directed along the same direction as $(\mathbf{Y}_{\tau,o} - \mathbf{X}_{\tau,o})$ but has length d_o. We then let the system evolve and obtain a distance, d_2, at the end of the second time step (see Fig. 2.6.2). We continue this process for n time steps, each of length τ. In so doing, we generate a sequence of distances, $\{d_j\}$, where $j = 1, \ldots, n$. The Lyapounov exponent is then

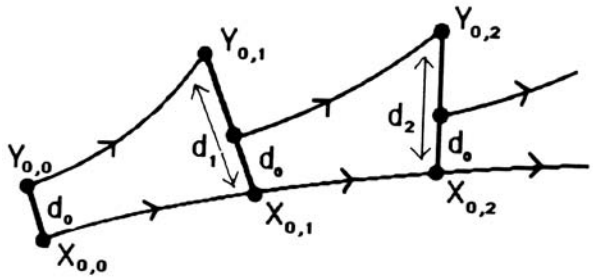

Figure 2.6.2. The Lyapounov exponent, $k_n(\tau, \mathbf{X}_{o,o}, \mathbf{Y}_{o,o})$, is obtained by computing a sequence of distances, d_n, between our reference trajectory, $\mathbf{X}_t^N$, and a neighboring trajectory. Each distance is obtained after a finite time interval, τ. In this figure, $\mathbf{X}_{o,n} = \mathbf{X}_{n\tau}^N$. The neighboring trajectory is adjusted at the beginning of each interval to lie a distance d_o from $\mathbf{X}_{n\tau}^N$.

defined as

$$k_n(\tau, \mathbf{X}_{o,o}, \mathbf{Y}_{o,o}) = \frac{1}{n\tau} \sum_{j=1}^{n} \ln\left(\frac{d_j}{d_o}\right). \tag{2.6.5}$$

If d_o is not too big the quantity $k_n(\tau, \mathbf{X}_{o,o}, \mathbf{Y}_{o,o})$ has been found to have the following properties [Benettin et al. 1976] [Casartelli et al. 1976]:

1. $\lim_{n\to\infty} k_n(\tau, \mathbf{X}_{o,o}, \mathbf{Y}_{o,o}) = k(\tau, \mathbf{X}_{o,o}, \mathbf{Y}_{o,o})$ exists;

2. $k(\tau, \mathbf{X}_{o,o}, \mathbf{Y}_{o,o})$ is independent of τ;

3. $k(\tau, \mathbf{X}_{o,o}, \mathbf{Y}_{o,o})$ is independent of d_o;

4. $k(\tau, \mathbf{X}_{o,o}, \mathbf{Y}_{o,o}) = 0$ if $\mathbf{X}_{o,o}$ is chosen to lie in a regular region of the energy surface;

5. $k(\tau, \mathbf{X}_{o,o}, \mathbf{Y}_{o,o})$ is independent of $\mathbf{X}_{o,o}$ and is positive if $\mathbf{X}_{o,o}$ is chosen to lie in a chaotic region of the energy surface.

Therefore, in a chaotic region of the energy surface, we can write $k(E) = k(\tau, \mathbf{X}_{o,o}, \mathbf{Y}_{o,o})$. The quantity $k(E)$ obtained in this manner is the largest Lyapounov exponent, λ_{N-1}.

Benettin, Froeshle, and Scheidecker [Benettin et al. 1979] have shown that it is possible to compute all of the Lyapounov exponents for a particular model Hamitonian system with N ($N = 4, 5$) degrees of freedom. Meyer [Meyer 1986] has been able to show that for sufficiently smooth Hamiltonians there are at least $2N$ vanishing Lyapounov exponents if there are N independent isolating integrals of the motion. In Figs. 2.6.3 and 2.6.4, we show some of the results of Benettin et al., who computed the Lyapounov exponent and KS metric entropy for the Henon-Heiles system (see Fig. 2.3.2). In Fig. 2.6.3, the Lyapounov exponent, k_n, is computed for six different initial conditions, three taken from the chaotic region and three

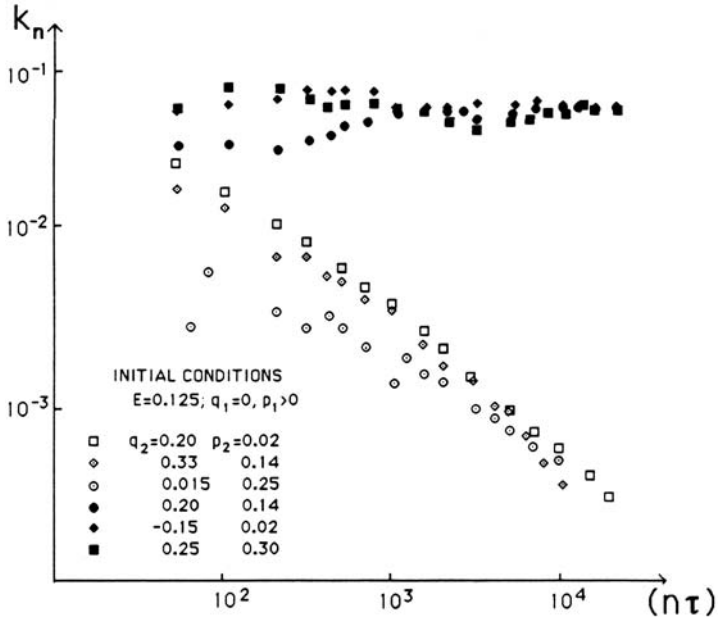

Figure 2.6.3. Plot of Lyapounov exponent k_n for the Henon-Heiles system for six different initial conditions, three chosen from the chaotic regime (black circle, diamond, and square) and three chosen from the regular regime (open circle, diamond, and square). For all initial conditions, the energy $E = 0.125$, and typically $d_o = 3 \times 10^{-4}$ and $\tau = 0.2$ (see Fig. 2.6.2). As $n \to \infty$, the exponent k_n approaches a positive constant value for trajectories in the chaotic regime, and approaches zero for trajectories in the regular regime. [Benettin et al. 1976]

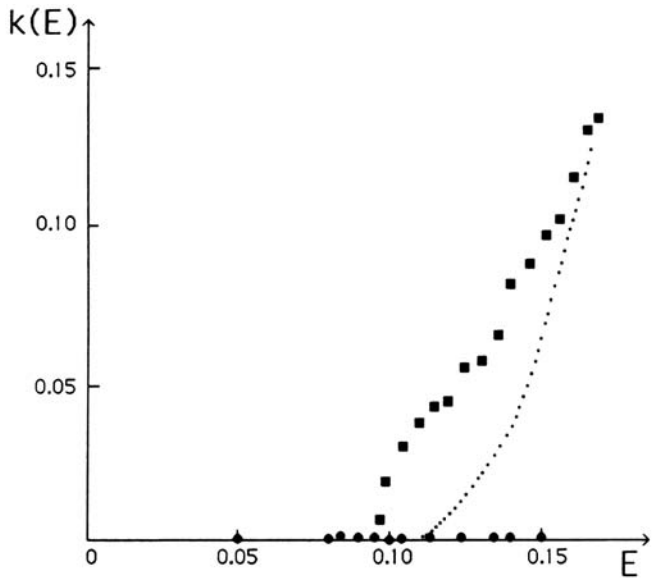

Figure 2.6.4. A plot of $k(E) = \lim_{n\to\infty} k_n$ as a function of energy for trajectories in the chaotic regime (black squares) and trajectories in the regular regime (black circles) of the Henon-Heiles system. The dotted line is an estimate of the KS metric entropy as a function of energy. [Benettin et al. 1976]

taken from the regular region (it is useful to locate these initial conditions in the surfaces of section for the Henon-Heiles system in Fig. 2.3.2). For initial conditions in the chaotic regime, all three exponents approach the same final value as $n \to \infty$, even though the initial conditions are taken from quite different regions of the phase space. For initial conditions in the regular region, the three exponents steadily decrease toward zero. In Fig. 2.6.4, the exponent $k(E) = \lim_{n\to\infty} k_n$ is plotted as a function of energy in both the chaotic and regular regimes for the Henon-Heiles system. The rate of divergence of trajectories appears to increase with increasing energy.

Regions of phase space for which neighboring trajectories have positive Lyapounov exponents are said to exhibit *sensitive dependence on initial conditions*, which is the definition of classical chaos. Any small change in the initial trajectories can lead to quite different final states.

2.6.2 KS Metric Entropy and K-Flows

There is a relation between the Lyapounov exponents and the KS metric entropy. In order to build some intuition about the KS metric entropy, let us consider the baker's map [Arnol'd and Avez 1968], [Penrose 1970],

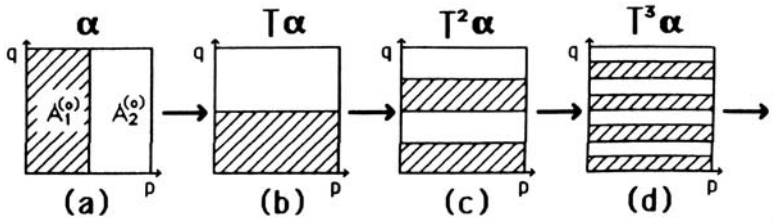

Figure 2.6.5. Behavior of the phase space of the unit square under the baker's map. The initial partition shown in (a) gets stretched into finer and finer filaments by the transformation, T.

[Reichl 1998], which is the simplest case of a Bernoulli shift [Moser 1973]. The baker's map consists of an alphabet with two "letters," 0 and 1, and the set, $\{S\}$, of all possible doubly infinite sequences

$$S = (\ldots, s_{-2}, s_{-1}, s_0; s_1, s_2, \ldots) \tag{2.6.6}$$

that can be formed from the alphabet by selecting $s_k = 0$ or 1, where s_k is the kth entry in the sequence and $-\infty \leq k \leq \infty$. The set $\{S\}$ includes sequences with random ordering and periodic ordering of elements. Each sequence, S, can be mapped to a point, (p, q), in the unit square by defining

$$p = \sum_{k=-\infty}^{0} s_k \; 2^{k-1} \tag{2.6.7}$$

and

$$q = \sum_{k=1}^{\infty} s_k \; 2^{-k}. \tag{2.6.8}$$

We can introduce dynamics into this system by means of the Bernoulli shift, T, which shifts all entries in a given sequence, S, to the right by one place. Let the sequence S be defined as in Eq. (2.6.6). Then

$$TS = (\ldots, s_{-3}, s_{-2}, s_{-1}; s_0, s_1, \ldots). \tag{2.6.9}$$

This shift causes the following mapping of the coordinates (p, q) on the unit square

$$T(p,q) = \begin{cases} (2p, \frac{1}{2}q) & \text{for} \quad 0 \leq p < \frac{1}{2} \\ (2p-1, \frac{1}{2}q + \frac{1}{2}) & \text{for} \quad \frac{1}{2} \leq p \leq 1 \end{cases} \tag{2.6.10}$$

It is important to note that whenever the element, s_0, of a sequence, S, has the value $s_0 = 0(1)$, the point (p, q) will lie to the left (right) of $p = \frac{1}{2}$. Thus, for random sequences, the point (p, q) will be mapped randomly to the left or right of $p = \frac{1}{2}$ by T.

Let us now introduce the partition of the unit square $\alpha = (A_1^{(0)}, A_2^{(0)})$ as shown in Fig. 2.6.5.a, where $A_i^{(0)}, i = 1, 2$ is an element of the partition, α.

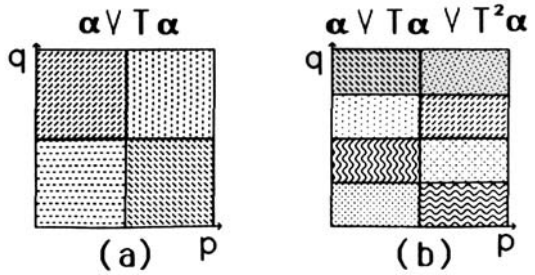

Figure 2.6.6. (a) The four elements of the partition resulting from the intersection of partitions α and $T\alpha$. (b) The eight elements of the partition resulting from the intersection of partitions α, $T\alpha$, and $T^2\alpha$. Each element is represented by a different pattern.

The effect of successive Bernoulli shifts will be to stretch the elements of this initial partition into filaments distributed throughout the unit square, as shown in Fig. 2.6.5. Let us next assign a measure, $p_i^{(0)} = \mu(A_i^{(0)})$, to the element $A_i^{(0)}$ $(i = 1, 2)$ equal to the fraction of the area of the unit square that it occupies. Then $\sum_{i=1}^{2} p_i^{(0)} = 1$. Thus, the measure of an element is the area that it occupies. From Fig. 2.6.5, we see that $T^n\alpha$ will contain 2^n elements, $T^n\alpha = (A_1^{(n)}, \ldots, A_{2^n}^{(n)})$. Let us next introduce the partition $\alpha \vee T\alpha$, which consists of elements $A_i^{(0)} \cap A_j^{(1)}$ $(i, j = 1, 2)$, where $\cap$ denotes the intersection of the elements $A_i^{(0)}$ and $A_j^{(1)}$. The partition $\alpha \vee T\alpha$ is shown in Fig. 2.6.6.a. Similarly. the elements of the partition $\alpha \vee T\alpha \vee T^2\alpha$ are shown in Fig. 2.6.6.b.

The KS metric entropy can now be defined as

$$h_{KS}(T) = \sup h(\alpha, T) = \sup \lim_{n\to\infty} \frac{h(\alpha \vee T\alpha \vee \ldots \vee T^{n-1}\alpha)}{n}, \qquad (2.6.11)$$

where

$$h(\alpha) = -\sum_i p_i \ \ln(p_i) \qquad (2.6.12)$$

and the sum is taken over all elements of partition α. The maximum value of the entropy occurs when the elements of a partition all have equal area. If we assume that our partitions do have equal area, then it is easy to see that

$$h(\alpha \vee T\alpha \vee \ldots \vee T^{n-1}\alpha) = -\sum_{i=1}^{2^n} \left(\frac{1}{2}\right)^n \ln\left[\left(\frac{1}{2}\right)^n\right] = n \ \ln(2). \qquad (2.6.13)$$

Thus, for the baker's map,

$$h_{KS}(t) = \ln(2). \qquad (2.6.14)$$

This analysis can be extended to Bernoulli shifts with an alphabet with k "letters." In that case, the KS metric entropy is $\ln(k)$. Therefore, the baker's map and Bernoulli shifts in general are K-flows. The dynamics contains contraction in the q direction and stretching in the p direction, very much like the flow in the neighborhood of a hyperbolic fixed point.

The connection between the Lyapounov exponents and the KS metric entropy was established by Piesin [Piesin 1976]. The KS metric entropy may be related to the Lyapounov exponents in the following way. Let

$$\rho(\mathbf{X}^N) = \sum_{i=1}^{N-1} \lambda_i(\mathbf{X}^N), \tag{2.6.15}$$

where $\lambda_i(\mathbf{X}^N)$ denotes the Lyapounov exponent in a region of phase space in the interval $\mathbf{X}^N \to \mathbf{X}^N + d\mathbf{X}^N$ on the energy surface. (Remember that the Lyapounov exponents are constant and nonzero throughout a stochastic region and are zero in regular regions.) The KS entropy is then [Benettin et al. 1979]

$$h(E) = \int_{\Gamma_E} \rho(\mathbf{X}^N) d\mu_E, \tag{2.6.16}$$

where $d\mu_E$ denotes an invariant volume element of the energy surface. Thus the KS entropy is directly related to the Lyapounov exponents. Benettin et al. [Benettin et al. 1976] have made an estimate of the KS metric entropy as a function of energy for the Henon-Heiles system. Their result, the dotted line, is shown in Fig. 2.6.4. The KS metric entropy has an energy dependence and qualitative behavior similar to that of the largest Lyapounov exponent for this system.

The Henon-Heiles system is one whose phase space contains a mixture of regular and chaotic trajectories. The fraction of the phase space occupied by each can be varied by varying parameters of the system. This is the most common type of behavior found in Hamiltonian systems and is characteristic of systems with smooth differentiable Hamiltonians.

One of the few systems that is known to be a K-flow for all values of its parameters is the hard sphere gas. This was proven by Sinai [Sinai 1963b] for the *Sinai billiard*, which consists of a particle confined in a box that has periodic boundary conditions and a hard circular barrier placed inside the box (see Fig. 2.6.7). The Hamiltonian of this system is not smooth and differentiable. The convex surface of the barrier causes neighboring trajectories to exponentially diverge from one another in phase space.

Let us now consider the dynamics of the Sinai billiard [Berry 1978]. Since the box has periodic boundary conditions, we may also view this system as that of a particle moving through a lattice of circular barriers. Assume that the average distance traveled between collisions with the barriers is D and the radius of the pillars is R. If two neighboring trajectories (we assume they have the same velocity) strike a barrier at points a distance ΔS_0 apart,

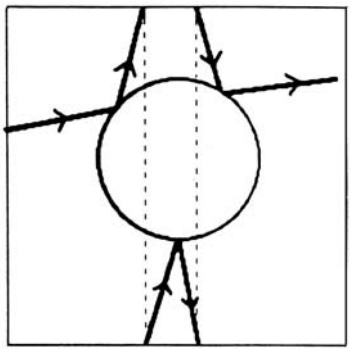

Figure 2.6.7. Sinai [Sinai 1963b] proved that the phase space flow of a moving particle confined to a box containing a hard circular barrier is a K-flow. The box is assumed to have periodic boundary conditions.

the angular distance will be $\Delta\theta_0 = \Delta S_0/R$ (see Fig. 2.6.8). However, when they strike the next barrier a distance D away, their points of collision will be separated a distance $\Delta S_1 \approx \Delta\theta_0 D$, and the angular separation of the collision points will be $\Delta\theta_1 \approx \frac{D}{R}\Delta\theta_0$. If we continue this process for n collisions, the approximate angular spread of points of collision will be $\Delta\theta_n \approx \left(\frac{D}{R}\right)^n \Delta\theta_0$. The number of collisions, n, needed for a divergence of one radian is $n = \ln(\Delta\theta_0)/\ln\left(\frac{R}{D}\right)$. It is interesting to consider an example. Let $\Delta\theta_0 = 0.0001$ radians and $R/D = 0.1$. Then $n = 4$ and it requires only four collisions to achieve a divergence of one radian.

Another system that has been proven to be a K-flow is that of a billiard moving in a planar concave region called a stadium. The stadium billiard consists of two half circles of radius r connected by equal parallel line segments of length $2a$ (see Fig. 2.6.9). When $a = 0$ and the system is circular, the motion of the billiard is integrable. However, for $a > 0$, it becomes a K-flow, as was proved by Bunimovich [Bunimovich 1974]. It should be noted, however, that Benettin and Strelcyn [Benettin and Strelcyn 1978] have found a transition region from regular to chaotic flow for $a \ll r$. We will return to the stadium billiard when we discuss quantum systems.

2.7 Time-Dependent Hamiltonians

Systems with time-dependent Hamiltonians of the form $H(p_1, \ldots, p_N; q_1, \ldots, q_N; t)$ that are periodic in time have proven most fruitful in studying the transition to chaos because with these systems it is often easiest to control the conditions under which the transition to chaos occurs. Because the dynamics of such systems is governed by Hamilton's equations, the

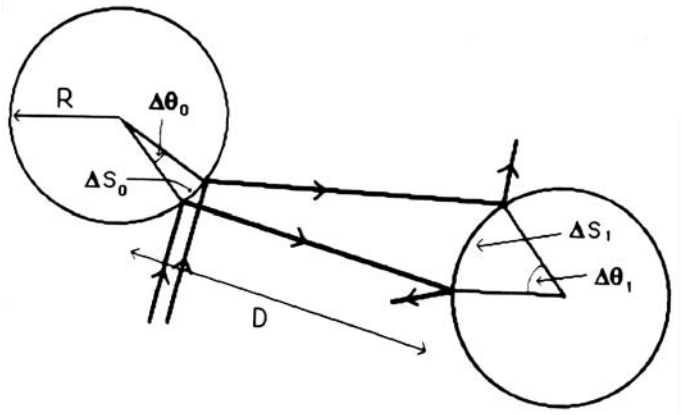

Figure 2.6.8. The phase space of a hard sphere gas is a K-flow. Neighboring trajectories diverge rapidly due to collisions with the hard convex surfaces.

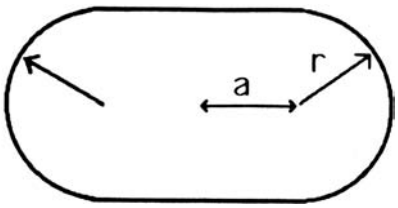

Figure 2.6.9. The stadium billiard is a two-dimensional billiard with spherical ends of radius r separated by parallel sides of length $2a$. For $a = 0$, the motion of a billiard is integrable, but for $a > 0$ it is a K-flow [Bunimovich 1974].

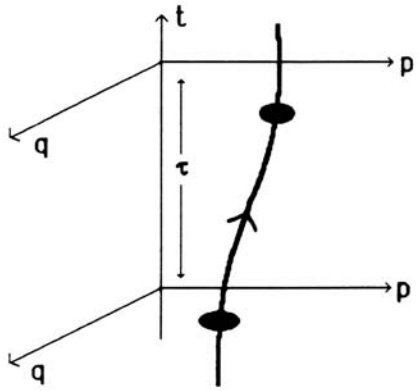

Figure 2.7.1. For a Hamiltonian that is periodic in time, a Poincaré surface of section can be obtained by plotting p and q at each period, τ, of the external field. This is sometimes called a strobe plot.

phase space flow is volume-preserving. In a higher-dimensional phase space, such systems are conservative. An N degree of freedom system with a time-periodic Hamiltonian, $H(p_1, \ldots, p_N; q_1, \ldots, q_N; t)$, is equivalent to an $N+1$ degree of freedom system with Hamiltonian

$$\mathcal{H}(p_1, \ldots, p_{N+1}; q_1, \ldots, q_{N+1}) = H(p_1, \ldots, p_N; q_1, \ldots, q_N; q_{N+1}) + p_{N+1}. \tag{2.7.1}$$

If the Hamiltonian is a periodic function of the time t, i.e.,

$$H(p_1, \ldots, p_N; q_1, \ldots, q_N; t) = H(p_1, \ldots, p_N; q_1, \ldots, q_N; t + \tau),$$

then the time plays a role analogous to that of an angle variable.

For a time-periodic Hamiltonian system with one degree of freedom, $H(p, q, t) = H(p, q, t+\tau)$, where τ is the period of the system, the Poincaré surface of section is just a strobe plot. That is, one simply plots (p, q) once every period τ (see Fig. 2.7.1). Nonlinear systems (not harmonic) with a Hamiltonian of the form

$$H(p, q, t) = H_0(p, q) + \epsilon H_1(p, q, t) \tag{2.7.2}$$

generally (but not always) fit the conditions of the KAM theorem. $H_0(p, q)$ describes an integrable system (all one degree of freedom systems are integrable), and $\epsilon H_1(p, q, t)$ is a perturbation, which can be made as small as we like by making ϵ small. Therefore, such systems are excellent candidates for studying the transition to chaos. Indeed, much of what we know about the transition has come from the study of such systems.

One of the simplest systems of this type is the conservative Duffing oscillator [Duffing 1918], [Davis 1962]. This system was first studied systematically by Duffing in 1918 and is one of the simplest model systems used for studying forced oscillations. The Duffing Hamiltonian may be written

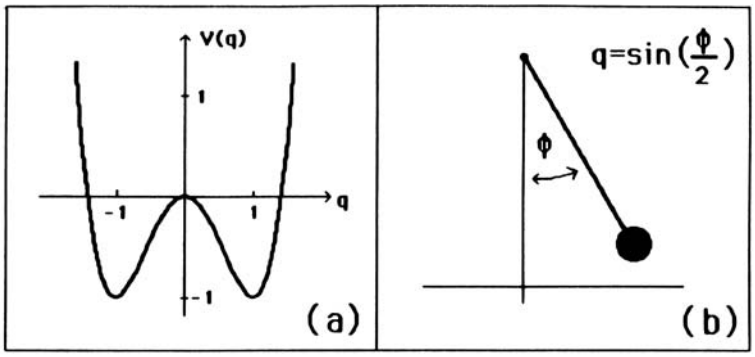

Figure 2.7.2. The conservative Duffing oscillator may be used to describe (a) the motion of a particle in a double-well potential, $V(q) = -2q^2 + q^4$, driven by a periodic external force, or (b) a pendulum driven by an external field for which the angle of deviation from the vertical, ϕ, is related to q by $q = \sin(\frac{\phi}{2})$.

[Reichl and Zheng 1984a, 1984b]

$$H = \frac{p^2}{4} - 2q^2 + q^4 + \epsilon q \cos(\omega_o t). \tag{2.7.3}$$

The equations of motion are

$$\frac{dp}{dt} = 4q - 4q^3 + \epsilon \cos(\omega_o t) \tag{2.7.4}$$

and

$$\frac{dq}{dt} = \frac{p}{2}. \tag{2.7.5}$$

These equations may be thought to describe either the motion of a particle in a double-well potential driven by a periodic external force or, if we make the change of variables $q = \sin(\frac{\phi}{2})$, that of a pendulum in the presence of an external driving force (see Fig. 2.7.2). The driven pendulum was also studied in [Lin and Reichl 1985].

For $\epsilon = 0$, this system is integrable, but for $\epsilon > 0$ it is nonintegrable. The external field induces nonlinear resonances into the phase space, and in regions where these resonances overlap, the phase space flow contains chaotic trajectories. The size and distribution of the resonances are determined by the structure of the unperturbed double well Hamiltonian

$$H_0 = \frac{p^2}{4} - 2q^2 + q^4 = E_o. \tag{2.7.6}$$

A phase space plot of trajectories for the unperturbed system H_0 is given in Fig. 2.7.3. The phase space has two elliptic fixed points at energy $E_o = -1$ and coordinates $p = 0, q = \pm 1$, corresponding to states in which the particle is at rest in the two valleys, and a hyperbolic fixed point at energy $E = 0$ and coordinates $p = q = 0$, corresponding to states in which the particle is

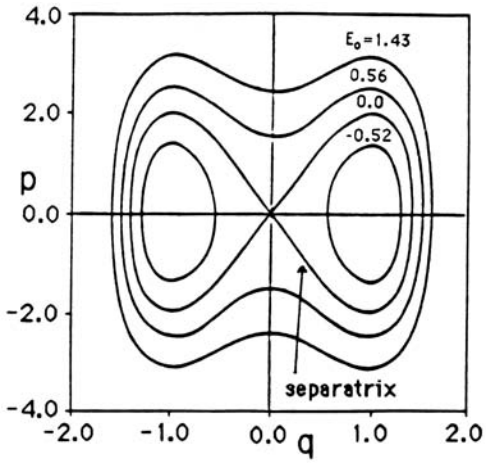

Figure 2.7.3. Phase space plot of trajectories for a system governed by the Hamiltonian $H_o = \frac{p^2}{4} - 2q^2 + q^4 = E_o$. A hyperbolic fixed point occurs at $p = q = 0$, and two elliptic fixed points occur at $p = 0, q = \pm 1$. [Reichl and Zheng 1984a]

at rest at the top of the hill (a point of unstable equilibrium). For energy $-1 < E_o < 0$, the particle is trapped in one of the two valleys. For energy $0 < E_o$, it is free to cross the barrier and roll back and forth between the two valleys. These two regions are separated by a separatrix.

We can perform a canonical transformation to action-angle variables (J, θ). The form of the canonical transformation is different for $-1 < E_o < 0$ and $0 < E_o$ because the motion is qualitatively different in those two regions. For $-1 < E_o < 0$ we find that the action is related to the energy via the equation (see Appendix B and [Reichl and Zheng 1984b, 1988])

$$J = \frac{4f}{3\pi}(\mathrm{E}(\kappa) - e^2\mathrm{K}(\kappa)), \tag{2.7.7}$$

where f and e are the outer and inner turning points of the trajectory, $\mathrm{K}(\kappa)$ and $\mathrm{E}(\kappa)$ are the complete elliptic integrals of the first and second kinds, respectively, and κ is the modulus. The modulus is defined as $\kappa^2 = \frac{f^2 - e^2}{f^2}$, and the turning points are defined as $f^2 = 1 + \sqrt{1 + E_o}$ and $e^2 = 1 - \sqrt{1 + E_o}$. Thus, in principle Eq. (2.7.7) can be reverted to obtain E_o as a function of J (i.e., $E_o = E_o(J)$), although in practice this generally is not possible. The relation between coordinates (p, q) and (J, θ) is given by

$$q = f \ \mathrm{dn}\left(\frac{\mathrm{K}(\kappa)\theta}{\pi}, \kappa\right) \tag{2.7.8}$$

and

$$p = 2f^2\kappa^2 \ \mathrm{sn}\left(\frac{\mathrm{K}(\kappa)\theta}{\pi}, \kappa\right) \ \mathrm{cn}\left(\frac{\mathrm{K}(\kappa)\theta}{\pi}, \kappa\right), \tag{2.7.9}$$

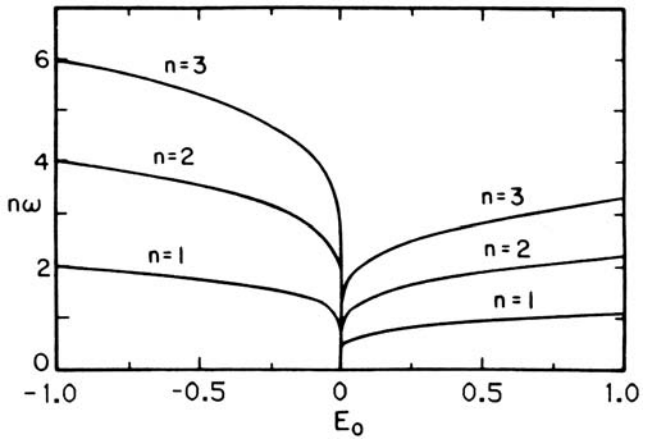

Figure 2.7.4. Plot of the natural frequency, ω, and its harmonics, $n\omega$ (for $n = 1, 2, 3$), of the unperturbed system as a function of energy, E_o. Note that the frequencies all approach zero at the separatrix.

where dn, sn, and cn are Jacobi elliptic functions [Byrd and Friedman 1971]. The canonical transformation between (p, q) and (J, θ) can be found in Appendix B and [Reichl and Zheng 1984b].

We can obtain the frequency of a given trajectory as a function of its action from Eq. (2.7.6). After some algebra, we obtain

$$\omega = \frac{\partial E_o}{\partial J} = \frac{f\pi}{\mathrm{K}(\kappa)}. \tag{2.7.10}$$

The time series for the position, q, or momentum, p, will contain contributions from all harmonics of this frequency. On a given trajectory, J is constant and $\theta = \omega t + \theta_o$, where θ_o is the initial angle. If we use these equations and expand Eq. (2.7.8) in a Fourier series [Byrd and Friedman 1971], we find

$$q(t) = \frac{f\pi}{2\mathrm{K}(\kappa)} + \frac{f\pi}{\mathrm{K}(\kappa)} \sum_{n=1}^{\infty} \operatorname{sech}\left(\frac{n\pi \mathrm{K}'(\kappa)}{\mathrm{K}(\kappa)}\right) \cos(n\omega t), \tag{2.7.11}$$

where $\mathrm{K}'(\kappa) = \mathrm{K}(\sqrt{1-\kappa^2})$. When we turn on the external field, it can resonate with all the harmonics, $n\omega$. Note that ω is a function of the energy, E_o, so as we vary the energy, the resonance frequency changes. Therefore these are nonlinear resonances.

It is useful to plot the frequencies $n\omega$ as a function of the energy E_o. The results are shown in Fig. 2.7.4. We see that the frequencies tend to zero in the neighborhood of the separatrix, and they all accumulate there. Thus, in the neighborhood of the separatrix, there are an infinite number of resonance zones. These can be seen explicitly if we rewrite the Hamiltonian

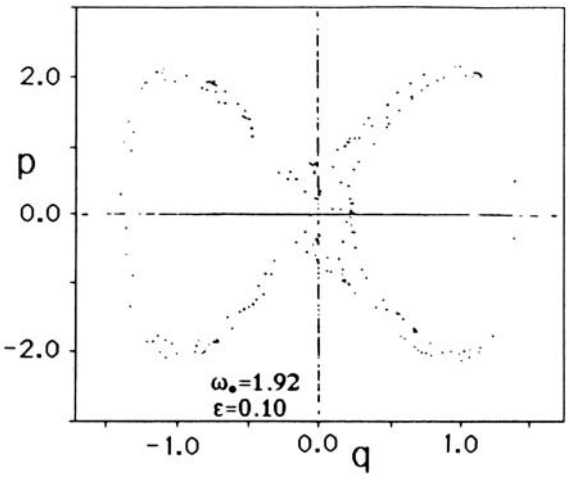

Figure 2.7.5. Strobe plot of the neighborhood of the separatrix shown in Fig. 2.7.3 for $\epsilon = 0.10$ and frequency $\omega_o = 1.92$. The separatrix is an accumulation point for resonance zones and will always contain chaotic orbits for $\epsilon > 0$. [Reichl and Zheng 1984a]

H in terms of action-angle variables. We then find

$$H = E_o(J) + \epsilon \sum_{n=-\infty}^{\infty} g_n(J) \cos(n\theta - \omega_o t), \tag{2.7.12}$$

where

$$g_n(J) = \frac{\pi}{2\mathrm{K}(\kappa)} \left(\frac{2}{2-\kappa^2} \right)^{\frac{1}{2}} \operatorname{sech} \left(\frac{n\pi \mathrm{K}'(\kappa)}{\mathrm{K}(\kappa)} \right). \tag{2.7.13}$$

Each traveling cosine wave in Eq. (2.7.12) gives rise to a nonlinear primary resonance zone. Phase space trajectories that have the same speed as a given cosine wave will be trapped by it and will cause a distortion of the phase space similar to that caused by the resonances in the Walker-Ford models in Sect. 2.4. The condition for trapping is that the speed of a trajectory, $\dot{\theta} = \omega$, be equal to the speed of a cosine wave, $\dot{\theta} = \frac{\omega_o}{n}$. Thus, at values of J that satisfy the resonance condition (f and K are functions of J)

$$\frac{f\pi}{\mathrm{K}(\kappa)} = \frac{\omega_o}{n}, \tag{2.7.14}$$

we will have a primary resonance zone. From Fig. 2.7.4, we see that we will always have an infinite number of resonances in the neighborhood of the separatrix regardless of the frequency, ω_o.

In Fig. 2.7.5, we show a strobe plot of the neighborhood of the separatrix. The external field frequency is $\omega_o = 1.92$ and the coupling constant $\epsilon =$

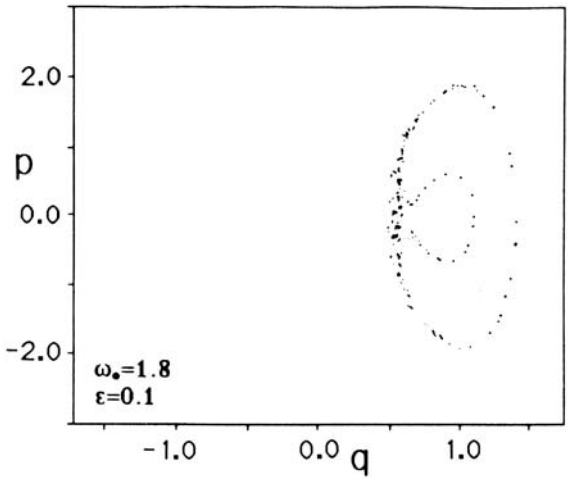

Figure 2.7.6. Strobe plot of the $n = 1$ primary resonance zone induced by the external field. At frequency $\omega_o = 1.8$, it lies well away from the unperturbed separatrix. Note that the separatrix of this primary resonance is also chaotic. [Reichl and Zheng 1984b]

0.10. The neighborhood of the separatrix will always be chaotic due to the infinite number of resonances that have accumulated there. Note that for $\epsilon \neq 0$ the unperturbed energy, E_o, for this trajectory is time dependent and oscillates chaotically. For coupling constant $\epsilon = 0.10$, there are mostly KAM tori. From Fig. 2.7.3, we see that if we choose an external frequency $\omega_o \leq 2n$, we should see a resonance zone lying at low energy. The $n = 1$ primary resonance zone is shown in Fig. 2.7.6 for $\omega_o = 1.8$ and $\epsilon = 0.1$. Notice that the separatrix of this primary resonance is chaotic. This is an indication of the self-similarity that exists in such systems, as we shall show later.

2.8 Conclusions

In this chapter, we have introduced concepts and model systems that will recur repeatedly throughout the remainder of the book. For example, the Toda lattice will reappear in Chapter 6, where we describe techniques used to construct integrable quantum mechanical systems. The stadium and the bakers map will also reappear in Chapter 6, where their quantum analogs will be studied. The Duffing oscillator reappears in Chapter 3, where we use it to construct the whisker map, and it appears in Chapter 4, where we use it to test renormalization predictions.

It is interesting to note that Ramani, Grammaticos, and Bountis [Ramani et al. 1989] have described a method different from that of Sect. 2.3 to determine if a system is integrable. They study the singularities of the differential equations and categorize them in terms of those singularities. They conjecture that systems of equations with the Painlevi property (the only moving singularities are poles) are integrable.

In this book, we will not discuss ergodic theory, which is a theory that attempts to lay the dynamical foundations of statistical mechanics. Suffice it to say that systems, such as the Sinai billiard, that are globally K-flows are also ergodic and mixing. Excellent discussions about the relation between ergodic theory and dynamics may be found in [Farquhar 1964], [Arnol'd and Avez 1968], and [Ornstein 1974]. Shorter discussions may be found in [Farquhar 1972], [Lebowitz and Penrose 1973], and [Reichl 1989].

2.9 Problems

2.1. A particle of mass $m = 1$ is constrained to move along the x-axis in the presence of a cubic potential $V(x) = -4x + \frac{3}{2}x^2 + \frac{1}{3}x^3$. (a) Prove that the Hamiltonian is a constant of the motion. (b) Sketch the potential $V(x)$ versus x. (c) Sketch the flow of trajectories in the Hamiltonian (p, x) phase space. Locate any hyperbolic and elliptic fixed points. Sketch in any separatrices. (c) Solve the equations of motion in the neighborhood of any hyperbolic or elliptic fixed points. Find the slopes and rate of exponentiation of the eigenvectors in the neighborhood of the hyperbolic points and the angular frequency of oscillation in the neighborhood of the elliptic fixed points.

2.2. Repeat parts (a)−(c) of Problem 2.1 for the Hamiltonian $H = \frac{1}{2}p^2 - x - \frac{1}{2}x^2 + \frac{1}{4}x^4$.

2.3. Find explicit expressions (in terms of phase space variables) for the three independent global constants of the motion for the three-body Toda lattice whose Hamiltonian is given by Eq. (2.3.17).

2.4. Consider the (2,3) resonance of Walker and Ford (in Sect. 2.4), which has Hamiltonian

$$H = J_1 + J_2 - J_1^2 - 3J_1J_2 + J_2^2 + \beta J_1 J_2^{3/2} \cos(2\theta_1 - 3\theta_2) = E.$$

Make the canonical transformation from coordinates $(J_1, J_2, \theta_1, \theta_2)$ to coordinates $(I_1, I_2, \phi_1, \phi_2)$, where $J_1 = I_1 - \frac{2}{3}I_2$, $J_2 = I_2$, $\theta_1 = \phi_1$, and $\theta_2 = \phi_2 + \frac{2}{3}\phi_1$. (a) Prove that the fixed points for even n (see Sect. 2.4) are hyperbolic while those for odd n are elliptic. (b) For very small β, find the energy at which the fixed points first appear. (c) Use perturbation theory to compute the coordinates $(J_1(t), J_2(t), \theta_1(t), \theta_2(t))$ to first order in β. Show that it diverges in the neighborhood of the (2,3) resonance.

2.5. Repeat parts (a)−(c) in Problem 2.4 for the Hamiltonian $H = J_1 + J_2 - J_1^2 - 3J_1J_2 + J_2^2 + \beta J_1^2 J_2 \cos(4\theta_1 - 2\theta_2)$.

2.6. Consider a system described by the Hamiltonian

$$H = J_1^2 + 2J_1J_2 + J_2^2 - \epsilon\cos(2\theta_1 - 3\theta_2) = E.$$

Find analytic solutions to the equations of motion. Sketch the Poincaré surfaces of section in the (J_1, θ_1) plane and in the (J_2, θ_2) plane.

2.7. Find all period 3 orbits of the baker's map. Plot them in the (p, q) plane.

2.8. Consider a system described by the Hamiltonian $H = \frac{1}{4}p^2 + V\cos(x - 3t)$. Sketch the phase space trajectories of this system in the (p, x) plane. Locate the separatrix and the elliptic and hyperbolic fixed points in the (p, x) plane. Compute the maximum width of the region bounded by the separatrix. Convert the time-dependent problem into a time-independent problem, using the method of Sect. 2.7, and compute $p(t)$ to first order in the coupling constant, V.

2.10 References

Abarbanel, H. (1976): in *Studies in Math Physics*, edited by E. Lieb, B. Simon, and A.S. Wrightman, Princeton Series in Physics (Princeton University Press, Princeton, N.J.).

Arnol'd, V.I. (1963): Russ. Math. Surv. **18** 9; **18** 85.

Arnol'd, V.I. and Avez, A. (1968): *Ergodic Problems of Classical Mechanics* (W.A. Benjamin, New York).

Barrar, R. (1970): Celestial Mech. **2** 494.

Benettin, G., Galgani, L., and Strelcyn, J.M. (1976): Phys. Rev. A **14** 2338.

Benettin, G. and Strelcyn, J.M. (1978): Phys. Rev. A **17** 773.

Benettin, G., Froeshle, C., and Scheidecker, J.P. (1979): Phys. Rev. A **19** 2454.

Berry, M.V. (1978): AIP Conference Proceedings **46** (American Institute of Physics, New York), p. 16. Reprinted in [MacKay and Meiss 1987].

Bunimovich, L.A. (1974): Funct. Anal. Appl. **8** 254.

Byrd, P.F. and Friedman, M.D. (1971): *Handbook of Elliptic Integrals for Engineers and Scientists* (Springer-Verlag, Berlin).

Casartelli, M., Diana, E., Galgani, L., and Scotti, A. (1976): Phys. Rev. A **13** 1921.

Chirikov, B. (1979): Phys. Rep. **52** 263.

Date, E. and Tanaka, S. (1976): Prog. Theor. Phys. **55** 457; Prog. Theor. Phys. Suppl. **59** 107.

Davis, H.T. (1962): *Introduction to Nonlinear Differential and Integral Equations* (Dover, New York).

Duffing, G. (1918): *Erzwungene Schwingungen bei veranderlicher Eigenfrequenz* (Braunschweig, Vieweg).

Farquhar, I.E. (1964): *Ergodic Theory in Statistical Mechanics* (Wiley-Interscience, New York).

Farquhar, I.E. (1972): in *Irreversibility in the Many-Body Problem*, edited by J. Beil and J. Rae (Plenum Press, New York).

Flaschka, H. (1974): Phys. Rev. B **9** 1924.
Ford, J., Stoddard, D.S., and Turner, J.S. (1973): Prog. Theor. Phys. **50** 1547.
Goldstein, H. (1980): *Classical Mechanics* (Addison-Wesley, Reading, Mass.).
Henon, M. and Heiles, C. (1964): Astron. J. **69** 73.
Henon, M. (1974): Phys. Rev. B **9** 1921.
Kac, M. and van Moerbeke, P.(1975): Proc. Natl. Acad. Sci. U.S.A. **72** 2879.
Kolmogorov, A.N. (1954): Dokl. Akad. Nauk. SSSR **98** 527 (1954) (An English version appears in R. Abraham, *Foundations of Mechanics* (W.A. Benjamin, New York, 1967, Appendix D).
Kolmogorov, A.N. (1958): Dokl. Akad. Nauk SSSR **119** 861.
Kolmogorov, A.N. (1959): Dokl. Akad. Nauk SSSR **124** 754.
Lax, P.D. (1968): Commun. Pure Appl. Math. **21** 467.
Lebowitz, J.L. and Penrose, O. (1973): Physics Today, February Issue.
Lichtenberg, A.J. and Lieberman, M.A. (1983): *Regular and Stochastic Motion* (Springer-Verlag, New York).
Lin, W.A. and Reichl, L.E. (1985): Phys .Rev. A **31** 1136.
MacKay, R.S. and Meiss, J.D. (1987): *Hamiltonian Dynamical Systems* (Adam Hilger, Bristol).
Meyer, H.D.(1986): J. Chem. Phys. **84** 3147.
Moser, J. (1962): Nachr. Akad. Wiss. Goettingen II, Math. Phys. Kd **1** 1.
Moser, J. (1970): Commun. Pure Appl. Math **23** 609.
Moser, J. (1973): *Stable and Random Motions in Dynamical Systems* (Princeton University Press, Princeton, N.J.).
Moser, J. (1979): Am. Sci. **67** 689.
Noether, E. (1918): Nach. Ges. Wiss. Goettingen **2** 235.
Ornstein, D.S. (1974): *Ergodic Theory, Randomness, and Dynamical Systems* (Yale University Press, New Haven).
Oseledec, V.I. (1968): Trans. Moscow Math. Soc. **19** 197.
Penrose, O. (1970): *Foundations of Statistical Mechanics* (Pergamon Press, Oxford).
Piesin, Ya.G. (1976): Math. Dokl. **17** 196.
Ramani, A., Grammaticos, B., and Bountis, T. (1989): Phys. Rep. **180** 159.
Reichl, L.E. (1998): *A Modern Course in Statistical Physics*, Second Edition (John Wiley and Sons, New York).
Reichl, L.E. and Zheng, W.M. (1984a): Phys. Rev. A **29** 2186.
Reichl, L.E. and Zheng, W.M. (1984b): Phys. Rev. A **30** 1068.
Reichl, L.E. and Zheng, W.M. (1988): in *Directions in Chaos*, edited by Hao Bai-lin (World Scientific, Singapore).
Sinai, Ya.G. (1963a): Am. Math. Soc. Transl. **31** 62.
Sinai, Ya.G. (1963b): Sov. Math. Dokl. **4** 1818.
Toda, M. (1967): J. Phys. Soc. Jpn. **22** 431; **23** 501.
Toda, M. (1981): *Theory of Nonlinear Lattices* (Springer-Verlag, Berlin)
Walker, G.H. and Ford, J. (1969): Phys. Rev. **188** 416.
Wintner, A. (1947): *The Analytical Foundations of Celestial Mechanics* (Princeton University Press, Princeton, N.J.).